1. Introduction

Alzheimer's disease (AD) is a major cause for dementia and has been considered to be a distinct entity from vascular dementia. However, recent pieces of evidence indicate a contribution of chronic cerebral hypoperfusion to the pathogenesis of AD. Indeed, reduction of cerebral blood flow (CBF) has been shown in temporal, parietal, and frontal cortices in the patients with AD (Waldemar et al., 1994; Johnson et al., 1998). This reduction of CBF has been attributed to reduced cerebral metabolism previously and may represent neurovascular coupling in response to an impaired synaptic activity.

However, several lines of evidence indicate dysregulation of regional CBF in AD brains, independent from derangement of synaptic activity. A decrease of CBF is documented even at early stages, indicating a microcirculatory insufficiency before the onset of AD pathology (Prohovnik et al., 1988). In addition, vascular networks in the cerebral cortices of AD patients are damaged and may contribute to the decrease of CBF (De Jong et al., 1997; Farkas et al., 2000; Kitaguchi et al., 2007), although it remains unclear whether these capillary damages are secondary to amyloid β (Aβ) deposition. Finally, in AD brains, there are frequent white matter (WM) lesions and cortical microinfarctions (Suter et al., 2002; Kovari et al., 2007), which are attributed to chronic cerebral hypoperfusion. In concordance with this microvascular derangement in AD, epidemiological data have revealed that vascular factors including mid-life hypertension and hyperlipidemia, diabetes mellitus, apo E4 genotype, are common risks for both AD and vascular dementia (Skoog et al., 1996; Launer et al., 2000; Kalaria, 2002; Kivipelto et al., 2006). Taken together, one can hypothesize that vascular factors and chronic cerebral hypoperfusion may accelerate AD pathology and cognitive decline.

However, there have been no data on whether chronic cerebral ischemia accelerates Aβ deposition in vivo, because the appropriate animal models have not been available. For this purpose, we successfully established a mouse model of chronic cerebral hypoperfusion, which exhibits mild cerebral hypoperfusion for an extended period and subsequently shows WM lesions and working memory deficits (Shibata et al., 2004; Shibata et al., 2007; Nakaji et al., 2006). In the present study, we applied chronic cerebral hypoperfusion to APP-Tg mouse and tested a possible alteration of Aβ metabolism.

2. Results

2.1. Histological stainings and immunohistochemistry

In the BCAS-treated mice at the age of 6 months and later, the WM was rarefied in the corpus callosum, caudoputamen, internal capsule and *anterior commissure* using Klüver-Barrera staining (Figs. 1A and B). However, there were no foci of cerebral infarctions in the cerebral cortices and the hippocampus. Using immunohistochemistry for GFAP, astroglia were much more numerous in the cerebral cortices, hippocampus, and WM such as the corpus callosum in the BCAS-treated mice at ages of 6, 9, and 12 months, as compared to those in the sham-operated mice (Figs. 1C and D).

Amyloid β_{1-40} immunostaining was observed occasionally in the vessel walls at 6 months and thereafter both in the mice with and without chronic cerebral hypoperfusion (Fig. 2A and B), whereas there were no obvious immunoreactivities in the neuronal somata for $A\beta_{1-42}$. There was no specific staining for $A\beta_{1-40}$ and $A\beta_{1-42}$ without the primary antibodies, and in the sections from wild-type mice which were subjected to either sham operation or BCAS. In the BCAS-treated mice at ages of 6, 9, and 12 months, there were neurons intensely immunoreactive for $A\beta_{1-42}$ with perinuclear staining, which may suggest accumulation of the antigen in the Golgi apparatus and multivesicular bodies, as compared to the sham-operated mice (Figs. 2C–H).

The numerical density of neurons with intensely immunoreactive for $A\beta_{1-42}$ were estimated in the representative 10 fields of 0.18 mm^2 from the cerebral cortex either sham-operated or BCAS-treated mice at ages of 12 months. Fig. 3A indicates an increase of these neurons with intense immunoreactivities for $A\beta_{1-42}$. The mouse model of chronic cerebral hypoperfusion does not exhibit focal necrosis or *atrophy* in the gray matter (Shibata et al., 2007). Similarly, in the gray matter, we did not observe any focal necrosis in the present study, but apoptotic cells significantly increased in number in the hippocampal CA1 and cerebral cortices even at ages of 12 months after BCAS (Figs. 3A and B). Therefore, one can postulate that intracellular accumulation of Aβ affects cellular metabolism and may have some relationship to apoptotic cell death, although it remains unclear whether these apoptotic neurons lead to significant reduction of neuronal density.

In the WM, including pencil fibers of the caudoputamen, optic tract and internal capsules, there were varicose fibers that were immunoreactive to antibodies against $A\beta_{1-42}$, whereas those immunoreactive for $A\beta_{1-40}$ were rarely found (Figs. 4A–D). Accumulation of $A\beta_{1-40}$ and $A\beta_{1-42}$ in the neuropil appeared occasionally in mice at the age of 7 months and constantly at 10 months, either with or without chronic cerebral hypoperfusion. With the antibody against $A\beta_{1-42}$, the immunoreactivity appeared as focal deposits surrounded by fibrillary deposits, whereas those for $A\beta_{1-40}$ were restricted to the round focal deposits, although the significance of differential pattern of amyloid deposits remained unclear (Figs. 4E and F). There were no differences in the distribution of $A\beta_{1-40}$ and $A\beta_{1-42}$ between the short-period group at ages of 12 months and the long-period group.

2.2. Western blot and filter assay

BCAS-treated mice showed the tendency to have higher levels of Aβ ($n=3$, $p=0.071$) in the extracellular-enriched brain fraction, as shown in the littermate pairs (a), (b), and (c) in the upper row of Fig. 5A. However, it did not reach statistical significance after correction by β-actin band density.

Next, we tested whether any structural changes in Aβ can be observed in chronic cerebral hypoperfusion with filter assay using ϕ200-nm nitrocellulose membrane, on which only the protein structures larger than 200 nm in diameter can be blotted. To validate the effectiveness of filter assay in specifically detecting Aβ fibrils, Aβ fibrils were prepared from synthetic $A\beta_{1-42}$ in vitro and subjected to filter assay as well as SDS-PAGE followed by the blotting, using anti-total Aβ

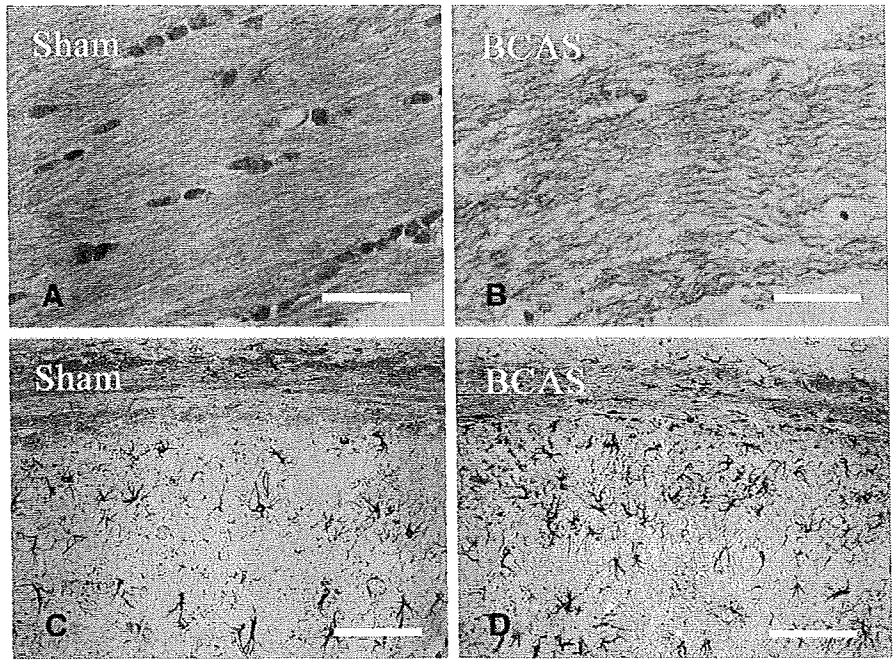

Fig. 1 – Photomicrographs of Klüver-Barrera staining (A, B) and immunohistochemistry for GFAP (C, D) in the corpus callosum (A, B) and the corpus callosum and hippocampal CA1 region (C, D) from the brains of sham-operated mice (A, C) and mice after chronic cerebral hypoperfusion (B, D). All mice were 12 months of age. Note the increase of GFAP-immunoreactive astroglia in both the corpus callosum and hippocampus. Scale bars indicate 50 μm.

(6E10) antibody (Fig. 5B). The Aβ fibrils formed after in vitro incubation were seen as high-molecular weight smear (Fig. 5B, asterisk [*]), which cannot be seen in the Aβ sample without incubation, whereas Aβ oligomers (Fig. 5B, asterisks [**]) and monomer (Fig. 5B, asterisks [***]) were detected with or without incubation. Conversely, in the filter assay, an Aβ-immunoreactive spot was seen only in the sample after incubation (Fig. 5B, bottom), indicating that monomers and oligomers had passed through the membrane.

Thus, we applied filter assay to the extracellular-enriched brain samples from the sham-operated and BCAS-treated mice. Interestingly, the Aβ-immmunoreactive spot density was increased *invariably* in the BCAS-treated mice, compared to the sham-operated mice (Fig. 5C), indicating that Aβ fibril formation was enhanced in the extracellular fraction after BCAS. Quantification of the spot density revealed that the increase was almost by 80% ($p=0.038$, $n=3$, Fig. 5D).

3. Discussion

In previous studies, increase of astroglia has been shown in the cerebral cortex and each part of the white matter in the BCAS-treated mice, along with rarefaction of the white matter (Shibata et al., 2004, 2007). The extent and distribution of glial activation in the present study correspond to those in previous reports and, therefore, indicate the same magnitude of ischemic insults after BCAS.

The altered metabolism of APP and Aβ has been indicated during in vitro hypoxia, and at multiple steps which favor the increase of APP and Aβ. Indeed, in human neuroblastoma cells, chronic hypoxia decreased the levels of α-secretase activity, which may upregulate Aβ production (Webster et al., 2002). In primary culture of neurons from human APP-Tg mice (Tg25769), hypoxia and glucose deprivation increased Aβ with a concomitant increase of γ-secretase and a delayed decrease of α-secretase, ADAM10 (Lee et al., 2006; Marshall et al., 2006). Hypoxia enhances the activity of β-secretase, the rate-limiting enzyme for Aβ production, in the cells expressing human APP695 (Zhang et al., 2007) and facilitates Aβ deposition and neuritic plaque formation in APP-Tg mice (Sun et al., 2006). More recently, neprilysin, metalloproteinase which degrades Aβ, has been shown to decrease in AD (Fisk et al., 2007).

In chronic cerebral ischemia, APP is accumulated in the neurites and soma of affected neurons (Wakita et al., 1992), being enhanced subcellularly in the endopalsmic reticulum and multivesicular bodies after transient global ischemia (Tomimoto et al., 1995). The increased cleavage of Aβ has been shown in a rat model of chronic cerebral hypoperfusion, but tissue deposition has not been demonstrated for Aβ (Bennet et al., 2000). In contrast, in focal cerebral ischemia, dense plaque-like APP deposits appear in the peri-infarct regions (van Groen et al., 2005).

These data collectively indicate that cerebral ischemia induces the abnormal metabolism of Aβ and may replicate the deposition of Aβ in AD. An altered metabolism in Aβ was shown in the present study after chronic cerebral hypoperfuion, but this mechanism remains unclear. β Secretase, β-site APP cleaving (BACE), is a membrane-bound aspartic protease, and the rate-limiting step in Aβ cleavage. Therefore, the Aβ

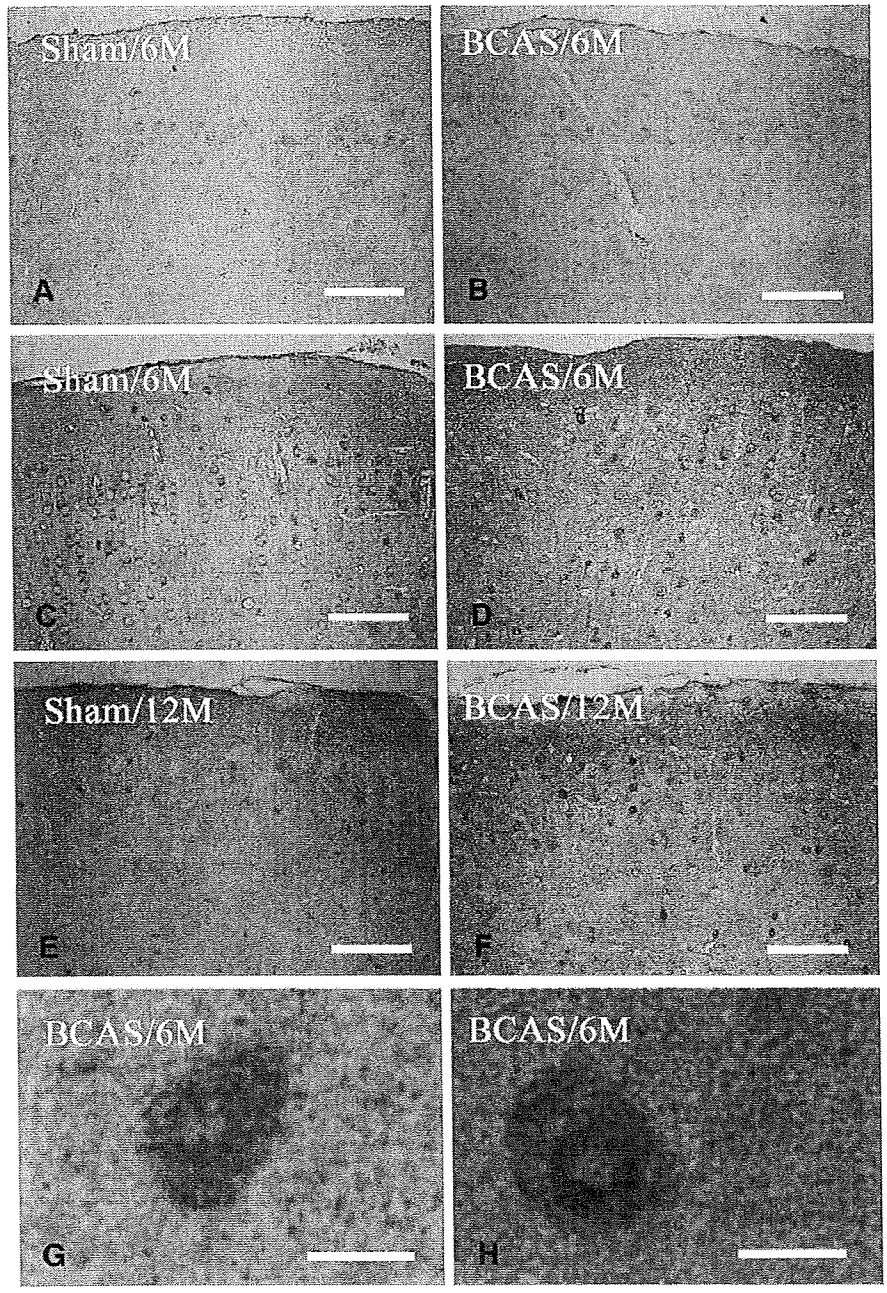

Fig. 2 – Photomicrographs of immunohistochemistry for $A\beta_{1-40}$ (A, B) and $A\beta_{1-42}$ (C–H) in the cerebral cortices. The mice were sham operated (A, C, E) and BCAS treated (B, D, F–H), and sacrificed at 6 months of age (A–D, G, H) and 12 months (E, F). Note that there are scattered intensely immunoreactive neurons, with enhanced immunostaining in the perinuclear regions. These neurons (H) were admixed with the neurons without perinuclear staining (G) in the cerebral cortices of BCAS-treated mice. Scale bars indicate 200 μm (A–F) and 10 μm (G, H).

load has been correlated with an increase in BACE activity in AD (Yang et al., 2003; Li et al., 2004; Chiocco et al., 2004; Johnston et al., 2005; Leuba et al., 2005). In aged APP-Tg mice, BACE was upregulated in the astroglia near amyloid plaques, suggesting that there may be Aβ production in the astroglia (Rossner et al., 2001). More recently, dysregulation in the intercompartmental transport of soluble Aβ has also been reported in AD with an increase in the receptors for advanced glycation end products (RAGE), thus transporting Aβ into the brain, and a decrease of low-density receptor-related protein (LRP)-1, which transports Aβ outside of the brain (Donahue et al., 2006). Chronic cerebral hypoperfusion may affect each of these processes of Aβ metabolism, and the exact mechanisms should be indicated in the future study.

Finally, it remains to be addressed in the future whether chronic cerebral hypoperfusion induces the abnormal

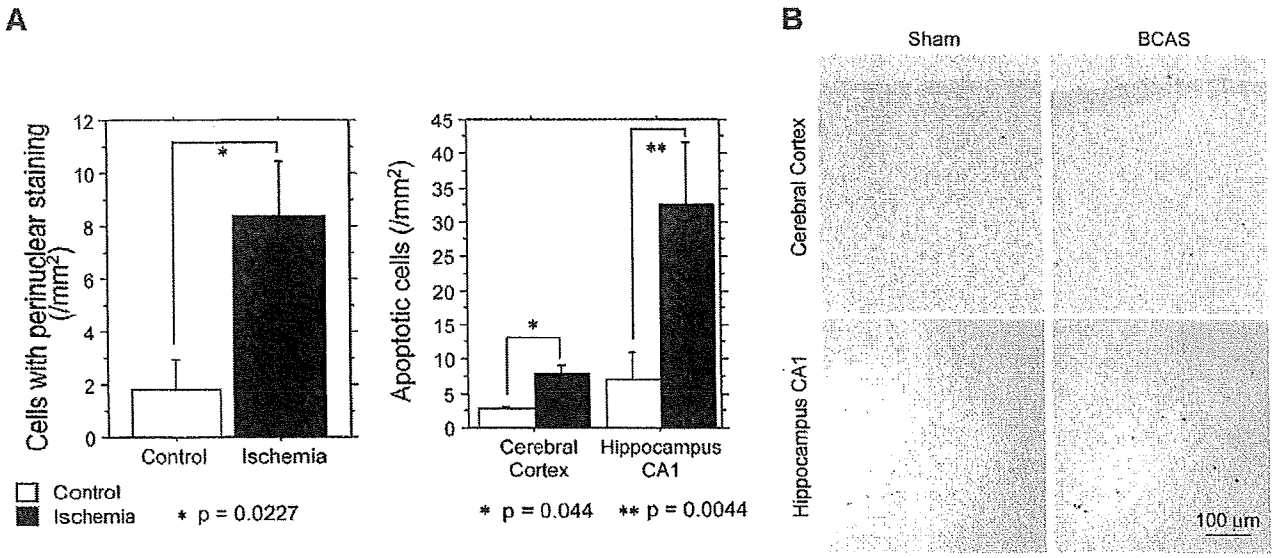

Fig. 3 – (A) Bar graphs showing the numerical density of cells with perinuclear staining and apoptotic cells. (B) Photomicrographs of TUNEL staining in the cerebral cortex and hippocampus in either sham-operated or BCAS-treated mice at 12 months of age.

phosphorylation of tau protein (Ikeda et al., 1998) and consequently accelerates synaptic dysfunction and cognitive deficits, since the Aβ load does not necessarily predict the magnitude of cognitive impairment (Giannakopoulos et al., 2003).

4. Experimental procedures

4.1. *Animals and treatments*

We used human APP-Tg mice overexpressing the familial AD-linked mutation carrying a mutant form of the human APP bearing the both Swedish (K670N/M671L) and the Indiana (V717F) mutations (APPSwInd) (Mucke et al., 2000), which has been imported from the Jackson Laboratory (USA). Mice were screened for transgene expression by PCR, and heterozygous mice were mated with nontransgenic C57BL/6J mice. All male heterozygous transgenic mice were given free access to food and water *ad libitum*. All procedures were performed in accordance with the guidelines for animal experimentation from the ethical committee of Kyoto University.

These mice were anesthetized with sodium pentobarbital intraperitoneally. Through a midline cervical incision, both common carotid arteries (CCAs) were exposed and freed from their sheaths. The microcoils, which were made of piano wire with an inner diameter of 0.18 mm, were constructed in Sawane Spring Co. (Japan). This microcoil was twined by rotating around the right CCA. After 30 min, another microcoil was twined around the left CCA. For the sham operation, the CCAs of the animals were exposed, but the microcoils were not twined.

Comparisons were then performed between APPSwInd transgenic mice and their littermates. At 5, 8, and 11 months of age, littermates of APP-Tg mice were subjected to either sham operation or bilateral carotid artery stenosis (BCAS) using microcoils (short-period group). One month after the sham operation or BCAS, these animals were examined. To test the effects of duration of chronic cerebral hypoperfusion, another batch of littermates of the APP-Tg mice were subjected to either sham operation or BCAS at 3 months of ages and were examined in the same manner after the survival for 9 months (long-period group). The long-period group was then compared to those operated at 11 months and sacrificed at 12 months.

4.2. *Histopathology and immunohistochemistry*

All animals were euthanized at 1 month and perfused transcardially with 0.01 mol/L phosphate-buffered saline (PBS) followed by 4% paraformaldehyde and 0.2% picric acid in 0.1 mol/L PBS (pH 7.4). The brains were removed and coronal brain blocks were postfixed for 24 h in 4% paraformaldehyde in 0.1 M PBS (pH 7.4) and then stored in 20% sucrose in 0.1 M PB (pH 7.4). Paraffin-embedded tissue was sectioned at 6-μm thickness. These sections were stained with hematoxylin and eosin (H & E) for examination of overall morphology and Klüver-Barrera staining for examination of the WM lesions.

For immunohistochemistry, the paraffin sections were incubated overnight at 4 °C with anti-glial fibrillary acidic protein (GFAP; Dakopatts, Denmark; diluted 1:1000). These sections were incubated with biotinylated anti-mouse IgG (Vector Laboratories, USA; diluted 1:200), and subsequently with avidin-biotin complex solution (Vector Laboratories; diluted 1:100). After each reaction, the sections were rinsed for 15 min with 0.1 M PBS. Finally, the immunoreaction products were visualized with a solution of 0.02% 3, 3′-diaminobenzidine tetrahydrochloride (DAB) and 0.005% H_2O_2 in 0.05 M Tris buffer (pH 7.6). Immunohistochemistry for $A\beta_{1-40}$ and $A\beta_{1-42}$ was performed using Aβ staining kit (Dakoppatts, Denmark) according to the manufacturer's recommendation.

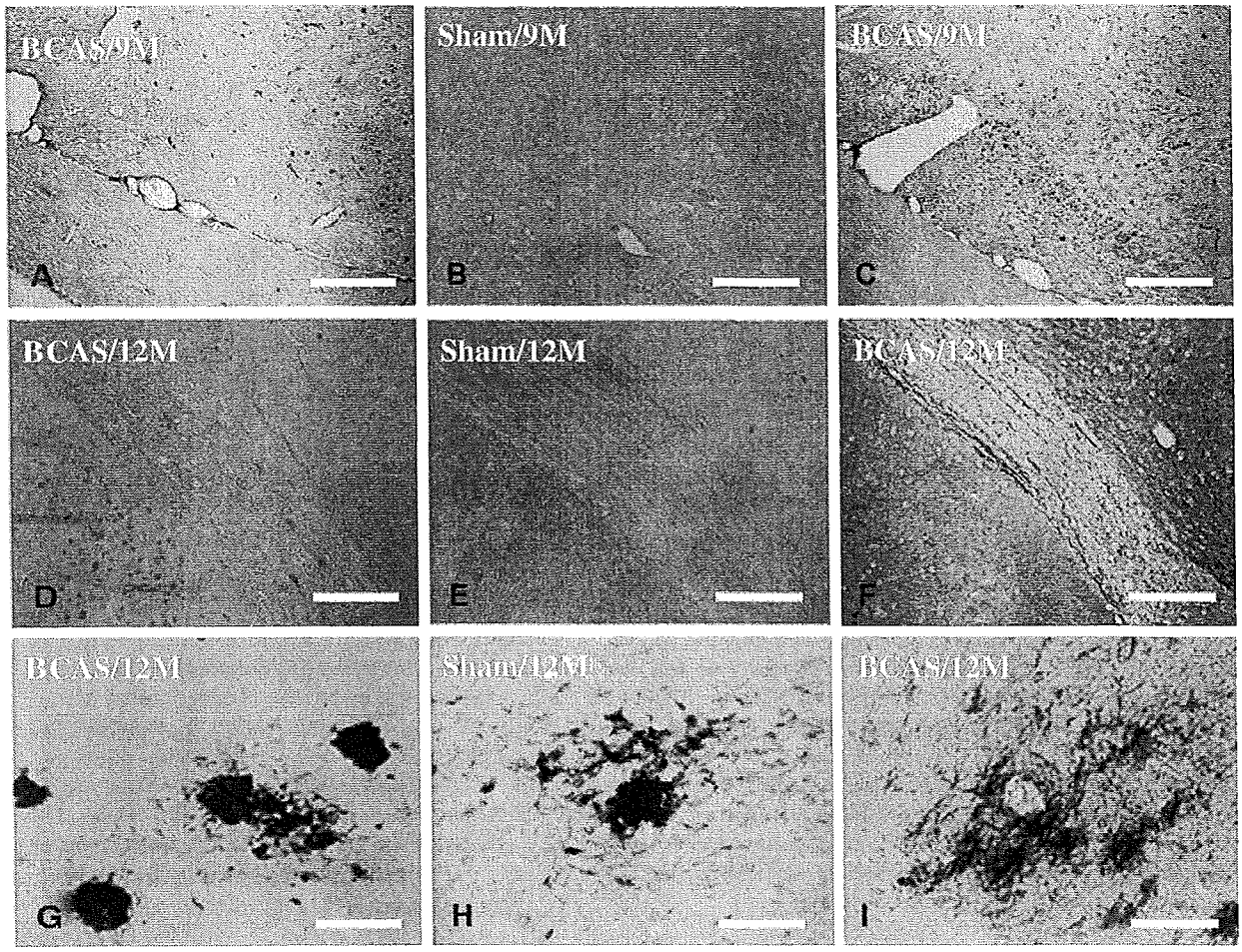

Fig. 4 – Photomicrographs of the immunohistochemistry for $A\beta_{1-40}$ (A, D, G) and $A\beta_{1-42}$ (B, C, E, F, H, I) in the internal capsule and optic tract (A–F) and the hippocampal CA3 region (G–I). Mice were sham treated (B, E, H) and BCAS treated (A, C, D, F, G, I) and sacrificed at 9 months of age (A–C) and 12 months (D–I). Scale bars indicate 500 μm (A–F) and 100 μm (G–I).

TUNEL staining was performed using the Apoptag in situ kit obtained from Oncor (Gaithersberg, MD, USA). After immersion in an equilibration buffer for 5 min, the sections were incubated with TdT and dUTP-digoxigenin in a humidified chamber at 37 °C for 1 h, and then incubated in the stop/wash buffer for 30 min. The sections were washed with 0.1 M PBS and incubated with an anti digoxigenin-peroxidase solution for 30 min. The sections were colorized with DAB-H_2O_2 solution as described above.

4.3. *Protein extraction*

The protein samples for Western blotting and the filter assay were extracted according to the method proposed by Lesne et al. (2006). Briefly, hemi-forebrains were harvested in 500 μL of solution containing 50 mM Tris–HCl (pH 7.6), 1% NP-40, 150 mM NaCl, 2 mM EDTA, 0.1% SDS, 1 mM phenylmethylsulfonyl fluoride (PMSF), and a protease inhibitor cocktail (Sigma, USA). Soluble, extracellular-enriched proteins were collected from mechanically homogenized lysates (1 mL syringe, gauge 20 needle [10 repeats]) following centrifugation for 5 min at 3000 rpm. The protein concentration of the samples was measured according to the Bradford (1976) method and equal amount of protein was subjected to Western blotting or filter assay.

4.4. *Western blotting and filter assay*

To examine the changes of APP metabolism in chronic cerebral hypoperfusion, we extracted the extracellular-enriched proteins from the brains of either sham-operated or BCAS-treated mice according to the protocol by Lesne et al., (2006). These mice were operated at the age of 8 months and sacrificed at the age of 9 months. Three pairs (pairs (a), (b), and (c)) of sham-operated or BCAS-treated mice were used for the analysis. Samples containing equal amounts of protein were diluted by Tricine SDS sample buffer (2×) (Invitrogen, USA) and electrophoresed on a 10%–20% Tricine gel (Invitrogen) in Tricine SDS Running Buffer (Invitrogen) according to the manufacturers' recommendation. Immunoblotting was performed by transferring the proteins to a PVDF membrane, blocking this membrane with 5% skimmed milk in Tris–HCl-buffered saline containing 1% TritonX-100 (TBS-T), and incubated with the primary antibody (6E10, Sigma; diluted

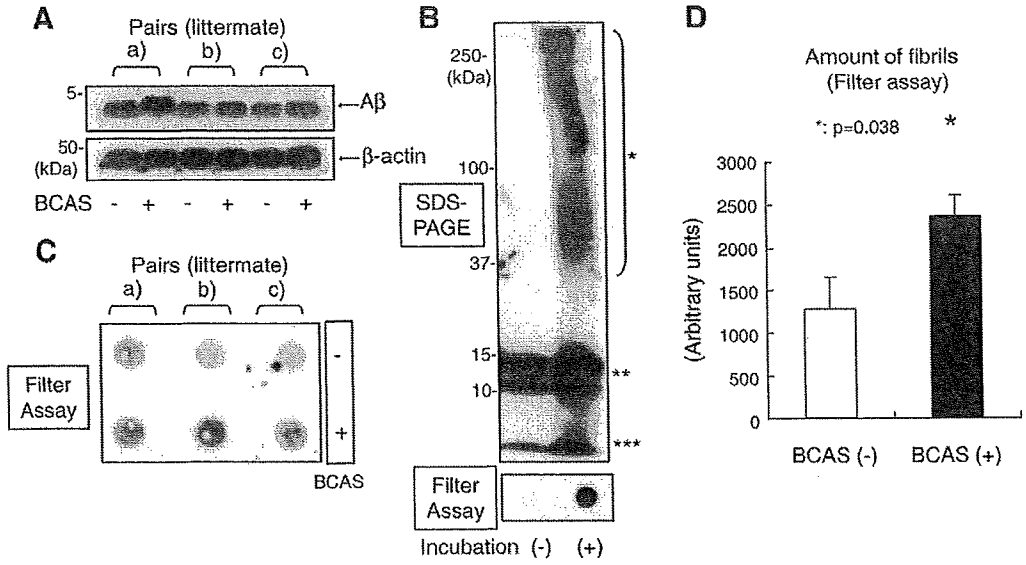

Fig. 5 – (A) Western blot of Aβ in the extracellular-enriched fraction of mouse brains using the anti-total Aβ (6E10) antibody. The lower panel indicates the bands of β-actin, which was used as a loading control. The Aβ fibrils were prepared in vitro from synthetic $A\beta_{1-42}$ and subjected to SDS-PAGE analysis (upper panel). (B) The Aβ fibril was seen as a high-molecular weight smear (') after incubation. The Aβ oligomers (**) and monomer (***) bands were seen both before and after incubation. The filter assay (bottom panel) demonstrated an Aβ immunopositive spot only after incubation, indicating that the Aβ monomer and oligomers passed through the membrane pore and failed to be blotted onto the membrane. (C) Extracellular-enriched protein samples obtained from brains of either BCAS-treated mice or sham-operated littermates were subjected to the filter assay. The Aβ-immunoreactive spot density was increased in the samples from BCAS-treated mice, as compared to their sham-operated littermates. (D) Statistical analysis of Aβ-immunoreactive spot density. The spot density was significantly increased in the samples obtained the BCAS-treated mice ($p=0.038$, $n=3$).

1:1000) in overnight at 4 °C. The membranes were then incubated with a HRP-linked anti-mouse IgG secondary antibody (GE Healthcare, UK; diluted 1:100) for 1 h at room temperature. The specific reaction was visualized, using the ECL method (GE Healthcare).

Protein samples from the brains of transgenic mice were subjected to vacuum filtration through a 96-well dot blot apparatus (Bio-Rad Laboratories, USA) containing ϕ200-nm nitrocellulose membranes. The resultant membranes were then incubated with primary antibody (6E10; diluted 1:1000) at 4 °C overnight. The membranes were then blocked by TBS-T containing 5% skim milk, and incubated with HRP-linked anti-mouse IgG secondary antibody (GE Healthcare; diluted 1:100) for 1 h. The membranes were developed with the ECL Western Blotting Analysis System (GE Healthcare).

Aβ fibrils for the positive control of the filter assay were prepared from synthetic $A\beta_{1-42}$ (Bachem AG, Switzerland). $A\beta_{1-42}$ was dissolved and brought to 100 μM in 0.1 M HCl and incubated at 37 °C, 24 h, for preparation of fibrils. Control Aβ monomer was dissolved in DMSO (100 μM) and used immediately after preparation. The samples were diluted by PBS into 1 μM and subjected to filter assay.

4.5. *Statistical analysis*

Data were expressed as mean±SEM except when otherwise noted. Statistical analyses were carried out by a one-way ANOVA followed by post hoc Fisher protected least significant differences test. A value of $p<0.05$ was considered statistically significant. Spots density obtained by the filter assay was quantified by the NIH image analyzer. All values are given in means±SD. Comparisons were performed using a paired Student's t-test. A $p<0.05$ was considered to indicate a significant difference.

Acknowledgments

This work was supported by a grant-in-aid for scientific research (C) (18590936) from the Japanese Ministry of Education, Culture, Sports and Technology. This study is a part of joint research, which is focusing on the development of the basis of technology for establishing COE for nano-medicine, carried out through Kyoto City Collaboration of Regional Entities for Advancing Technology Excellence assigned by Japan Science and Technology Agency (JST).

REFERENCES

Bennett, S.A., Pappas, B.A., Stevens, W.D., Davidson, C.M., Fortin, T., Chen, J., 2000. Cleavage of amyloid precursor protein elicited by chronic cerebral hypoperfusion. Neurobiol. Aging 21, 207–214.

Bradford, M.M., 1976. A rapid and sensitive method for the quantitation of microgram quantities of protein utilizing the principle of protein-dye binding. Anal. Biochem. 72, 248–254.

Chiocco, M.J., Kulnane, L.S., Younkin, L., Younkin, S., Evin, G., Lamb, B.T., 2004. Altered amyloid-beta metabolism and deposition in genomic-based beta-secretase transgenic mice. J. Biol. Chem. 279, 52535–52542.

De Jong, G.I., De Vos, R.A., Steur, E.N., Luiten, P.G., 1997. Cerebrovascular hypoperfusion: a risk factor for Alzheimer's disease? Animal model and postmortem human studies. Ann. N. Y. Acad. Sci. 826, 56–74.

Donahue, J.E., Flaherty, S.L., Johanson, C.E., Duncan III, J.A., Silverberg, G.D., Miller, M.C., Tavares, R., Yang, W., Wu, Q., Sabo, E., Hovanesian, V., Stopa, E.G., 2006. RAGE, LRP-1, and amyloid-beta protein in Alzheimer's disease. Acta. Neuropathol. (Berl). 112, 405–415.

Farkas, E., De Jong, G.I., Apro, E., De Vos, R.A., Steur, E.N., Luiten, P.G., 2000. Similar ultrastructural breakdown of cerebrocortical capillaries in Alzheimer's disease, Parkinson's disease, and experimental hypertension. What is the functional link. Ann. N. Y. Acad. Sci. 903, 72–82.

Fisk, L., Nalivaeva, N.N., Boyle, J.P., Peers, C.S., Turner, A.J., 2007. Effects of hypoxia and oxidative stress on expression of neprilysin in human neuroblastoma cells and rat cortical neurons and astrocytes. Neurochem. Res. 32, 1741–1748.

Giannakopoulos, P., Herrmann, F.R., Bussiere, T., Bouras, C., Kovari, E., Perl, D.P., Morrison, J.H., Gold, G., Hof, P.R., 2003. Tangle and neuron numbers, but not amyloid load, predict cognitive status in Alzheimer's disease. Neurology 60, 1495–1500.

Ikeda, K., Akiyama, H., Arai, T., Kondo, H., Haga, C., Iritani, S., Tsuchiya, K., 1998. Alz-50/Gallyas-positive lysosome-like intraneuronal granules in Alzheimer's disease and control brains. Neurosci. Lett. 258, 113–116.

Johnson, K.A., Jones, K., Holman, B.L., Becker, J.A., Spiers, P.A., Satlin, A., Albert, M.S., 1998. Preclinical prediction of Alzheimer's disease using SPECT. Neurology 50, 1563–1571.

Johnston, J.A., Liu, W.W., Todd, S.A., Coulson, D.T., Murphy, S., Irvine, G.B., Passmore, A.P., 2005. Expression and activity of beta-site amyloid precursor protein cleaving enzyme in Alzheimer's disease. Biochem. Soc. Trans. 33 (Pt 5), 1096–1100.

Kalaria, R., 2002. Similarities between Alzheimer's disease and vascular dementia. J. Neurol. Sci. 203-204, 29–34.

Kitaguchi, H., Ihara, M., Saiki, H., Takahashi, R., Tomimoto, H., 2007. Capillary beds are decreased in Alzheimer's disease, but not in Binswanger's disease. Neurosci. Lett. 417, 128–131.

Kivipelto, M., Ngandu, T., Laatikainen, T., Winblad, B., Soininen, H., Tuomilehto, J., 2006. Risk score for the prediction of dementia risk in 20 years among middle aged people: a longitudinal, population-based study. Lancet. Neurol. 5, 735–741.

Kovari, E., Gold, G., Herrmann, F.R., Canuto, A., Hof, P.R., Bouras, C., Giannakopoulos, P., 2007. Cortical microinfarcts and demyelination affect cognition in cases at high risk for dementia. Neurology 68, 927–931.

Launer, L.J., Ross, G.W., Petrovitch, H., Masaki, K., Foley, D., White, L.R., Havlik, R.J., 2000. Midlife blood pressure and dementia: the Honolulu-Asia aging study. Neurobiol. Aging 21, 49–55.

Lee, P.H., Hwang, E.M., Hong, H.S., Boo, J.H., Mook-Jung, I., Huh, K., 2006. Effect of ischemic neuronal insults on amyloid precursor protein processing. Neurochem. Res. 31, 821–827.

Lesne, S., Koh, M.T., Kotilinek, L., Kayed, R., Glabe, C.G., Yang, A., Gallagher, M., Ashe, K.H., 2006. A specific amyloid-beta protein assembly in the brain impairs memory. Nature 440, 352–357.

Leuba, G., Wernli, G., Vernay, A., Kraftsik, R., Mohajeri, M.H., Saini, K.D., 2005. Neuronal and nonneuronal quantitative BACE immunocytochemical expression in the entorhinohippocampal and frontal regions in Alzheimer's disease. Dement. Geriatr. Cogn. Disord. 19, 171–183.

Li, R., Lindholm, K., Yang, L.B., Yue, X., Citron, M., Yan, R., Beach, T., Sue, L., Sabbagh, M., Cai, H., Wong, P., Price, D., Shen, Y., 2004. Amyloid beta peptide load is correlated with increased beta-secretase activity in sporadic Alzheimer's disease patients. Proc. Natl. Acad. Sci. U.S.A. 101, 3632–3637.

Marshall, A.J., Rattray, M., Vaughan, P.F., 2006. Chronic hypoxia in the human neuroblastoma SH-SY5Y causes reduced expression of the putative alpha-secretases, ADAM10 and TACE, without altering their mRNA levels. Brain Res. 1099, 18–24.

Mucke, L., Masliah, E., Yu, G.Q., Mallory, M., Rockenstein, E.M., Tatsuno, G., Hu, K., Kholodenko, D., Johnson-Wood, K., McConlogue, L., 2000. High-level neuronal expression of abeta 1-42 in wild-type human amyloid protein precursor transgenic mice: synaptotoxicity without plaque formation. J. Neurosci. 20, 4050–4058.

Nakaji, K., Ihara, M., Takahashi, C., Itohara, S., Noda, M., Takahashi, R., Tomimoto, H., 2006. Matrix metalloproteinase-2 plays a critical role in the pathogenesis of white matter lesions after chronic cerebral hypoperfusion in rodents. Stroke 37, 2816–2823.

Prohovnik, I., Mayeux, R., Sackeim, H.A., Smith, G., Stern, Y., Alderson, P.O., 1988. Cerebral perfusion as a diagnostic marker of early Alzheimer's disease. Neurology 38, 931–937.

Rossner, S., Apelt, J., Schliebs, R., Perez-Polo, J.R., Bigl, V., 2001. Neuronal and glial beta-secretase (BACE) protein expression in transgenic Tg2576 mice with amyloid plaque pathology. J. Neurosci. Res. 64, 437–446.

Skoog, I., Lernfelt, B., Landahl, S., Palmertz, B., Andreasson, L.A., Nilsson, L., Persson, G., Oden, A., Svanborg, A., 1996. 15-year longitudinal study of blood pressure and dementia. Lancet 347, 1141–1145.

Sun, X., He, G., Qing, H., Zhou, W., Dobie, F., Cai, F., Staufenbiel, M., Huang, L.E., Song, W., 2006. Hypoxia facilitates Alzheimer's disease pathogenesis by up-regulating BACE1 gene expression. Proc. Natl. Acad. Sci. U.S.A. 103, 18727–18732.

Suter, O.C., Sunthorn, T., Kraftsik, R., Straubel, J., Darekar, P., Khalili, K., Miklossy, J., 2002. Cerebral hypoperfusion generates cortical watershed microinfarcts in Alzheimer disease Stroke 33, 1986–1992.

Shibata, M., Ohtani, R., Ihara, M., Tomimoto, H., 2004. White matter lesions and glial activation in a novel mouse model of chronic cerebral hypoperfusion. Stroke 35, 2598–2603.

Shibata, M., Yamasaki, N., Miyakawa, T., Kalaria, R.N., Fujita, Y., Ohtani, R., Ihara, M., Takahashi, R., Tomimoto, H., 2007. Selective impairment of working memory in a mouse model of chronic cerebral hypoperfusion. Stroke 38, 2826–2832.

Tomimoto, H., Akiguchi, I., Wakita, H., Nakamura, S., Kimura, J., 1995. Ultrastructural localization of amyloid protein precursor in the normal and postischemic gerbil brain. Brain Res. 672, 187–195.

van Groen, T., Puurunen, K., Maki, H.M., Sivenius, J., Jolkkonen, J., 2005. Transformation of diffuse beta-amyloid precursor protein and beta-amyloid deposits to plaques in the thalamus after transient occlusion of the middle cerebral artery in rats. Stroke 36, 1551–1556.

Wakita, H., Tomimoto, H., Akiguchi, I., Ohnishi, K., Nakamura, S., Kimura, J., 1992. Regional accumulation of amyloid beta/A4 protein precursor in the gerbil brain following transient cerebral ischemia. Neurosci. Lett. 146, 135–138.

Waldemar, G., Bruhn, P., Kristensen, M., Johnsen, A., Paulson, O.B., Lassen, N.A., 1994. Heterogeneity of neocortical cerebral blood flow deficits in dementia of the Alzheimer type: a [99mTc]-d, l-HMPAO SPECT study. J. Neurol. Neurosurg. Psychiatry 57, 285–295.

Webster, N.J., Green, K.N., Peers, C., Vaughan, P.F., 2002. Altered processing of amyloid precursor protein in the human neuroblastoma SH-SY5Y by chronic hypoxia. J. Neurochem. 83, 1262–1271.

Yang, L.B., Lindholm, K., Yan, R., Citron, M., Xia, W., Yang, X.L., Beach, T., Sue, L., Wong, P., Price, D., Li, R., Shen, Y., 2003. Elevated beta-secretase expression and enzymatic activity detected in sporadic Alzheimer disease. Nat. Med. 9, 3–4.

Zhang, X., Zhou, K., Wang, R., Cui, J., Lipton, S.A., Liao, F.F., Xu, H., Zhang, Y.W., 2007. Hypoxia-inducible factor 1alpha (HIF-1alpha)-mediated hypoxia increases BACE1 expression and beta-amyloid generation. J. Biol. Chem. 282, 10873–10880.

INTERNAL MEDICINE

□ CASE REPORT □

Leukoencephalopathy with Cognitive Impairment following Tocilizumab for the Treatment of Rheumatoid Arthritis (RA)

Katsuya Kobayashi[1], Yoko Okamoto[1], Haruhisa Inoue[1], Takashi Usui[2], Masafumi Ihara[1], Jun Kawamata[1], Yukio Miki[3], Tsuneyo Mimori[2], Hidekazu Tomimoto[4] and Ryosuke Takahashi[1]

Abstract

The biological agent tocilizumab, is a humanized, anti-human interleukin-6 receptor antibody. A 72-year-old woman developed cognitive impairment during the Phase III clinical trial of tocilizumab for the treatment of rheumatoid arthritis. MRI demonstrated hyperintense dissemination throughout the white matter on T2WI. An initial diagnosis of possible progressive multifocal leukoencephalopathy was made, but the PCR for JC virus DNA was negative in the CSF. The leukoencephalopathy might have been caused by a mechanism related to tocilizumab itself. It is strongly recommended to perform MRI if a patient develops any cognitive impairment during tocilizumab therapy.

Key words: rheumatoid arthritis, tocilizumab, leukoencephalopathy, cognitive impairment, MRI, interleukin 6

(Inter Med 48: 1307-1309, 2009)
(DOI: 10.2169/internalmedicine.48.1926)

Introduction

Tocilizumab is a humanized, anti-human interleukin-6 receptor antibody, produced by genetic engineering technology. To date, it has been prescribed solely to patients with Castleman disease. Phase III clinical trials of tocilizumab have already been performed on patients with rheumatoid arthritis. Here, we report the first case of leukoencephalopathy with cognitive impairment, likely caused by tocilizumab for the treatment of rheumatoid arthritis.

Case Report

A left-handed 72-year-old woman was referred to our hospital because her cognition had worsened over the previous two months. She had suffered from rheumatoid arthritis (RA) for the past six years, and since a daily dosage of 10 mg prednisolone had not been proved effective, it was decided that she participated in the Phase III clinical trial of tocilizumab. During the trial, the patient took 8 mg/kg of tocilizumab every four weeks. Forty months after commencing to take tocilizumab, she began to show signs of dementia and abnormal behavior. She became unable to check blood glucose by herself, put things in order, and speak coherently.

At the time she was admitted, her blood pressure was 124/64 mmHg, and her body temperature was 37.2℃. A physical examination revealed bilateral pretibial edema and ankylosis of several joints. She was orientated, but anxious and nervous. She was not able to concentrate, and showed cognitive dysfunction with a Mini-Mental State Examination (MMSE) score of 23 and a Frontal Assessment Battery (FAB) score of 8. Snout reflex and bilateral sucking reflexes were positive. There were no motor or sensory disturbances. Bilateral Achilles tendon reflexes were decreased. Laboratory investigation demonstrated normal blood cell counts.

[1]Department of Neurology, Kyoto University Hospital, Kyoto, [2]Department of Rheumatology and Clinical Immunology, Kyoto University Hospital, Kyoto, [3]Department of Diagnostic Imaging and Nuclear Medicine, Kyoto University Hospital, Kyoto and [4]Department of Neurology, Mie University Hospital, Tsu
Received for publication December 7, 2008; Accepted for publication March 22, 2009
Correspondence to Dr. Yoko Okamoto, yoko416@kuhp.kyoto-u.ac.jp

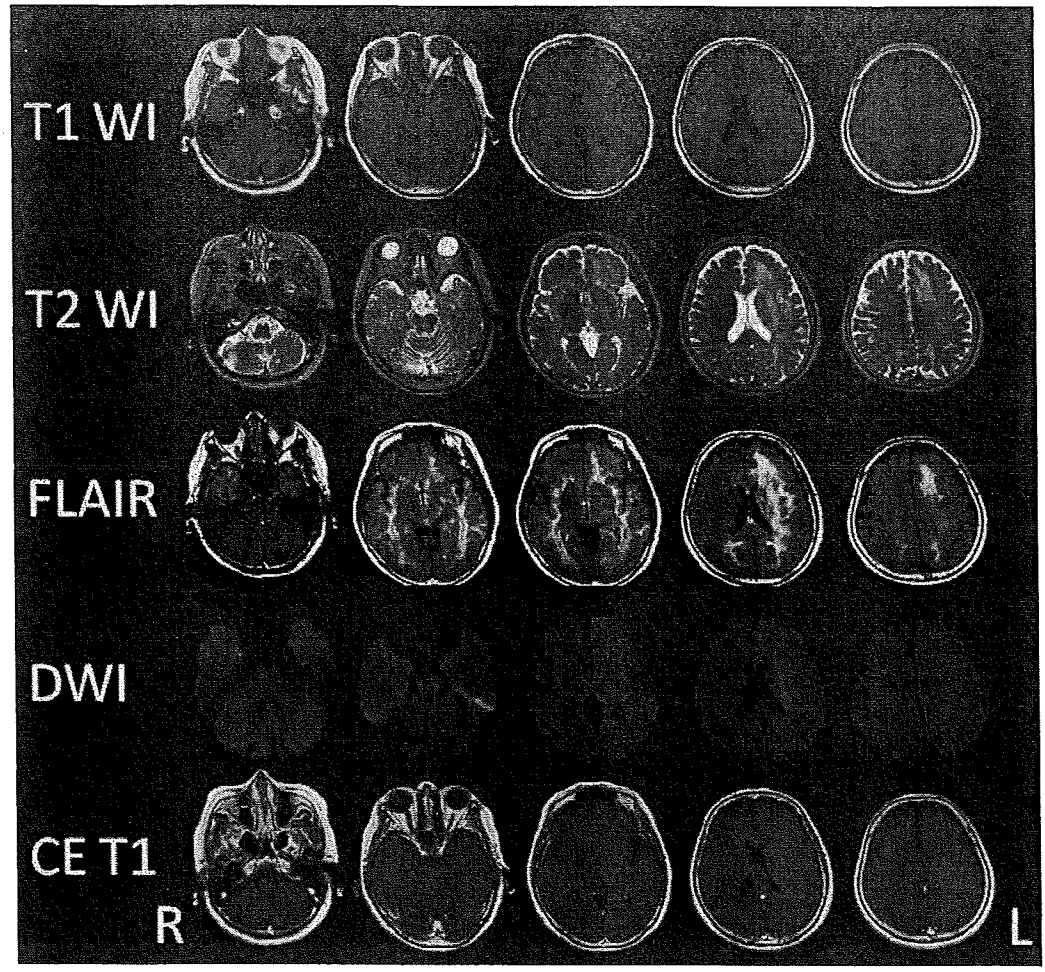

Figure 1. Brain MRI at the time of the admission. MRI disclosed high intensity dissemination throughout the white matter which spread widely from the temporal tip to the pars opercularis on T2WI and FLAIR. In accordance with the high intensity lesions on T2WI and FLAIR, slightly low intensity lesions were found on T1WI. There was no high intensity lesion on DWI except for T2 "shine-through" lesions of the left corona radiata. There was no mass effect or contrast enhancement lesion on contrast-enhanced T1WI.

Serum biochemistry showed an elevation of HbA1c (6.2%), anti-nuclear antibody, rheumatoid factor (RF, 62.3 IU/mL) and matrix metalloprotainase-3 (MMP-3, 215 ng/mL). The other autoimmune antibodies including anti-double stranded DNA, ribonucleoprotein, SS-A, SS-B, Scl-70, Jo-1, c-ANCA, p-ANCA, thyroid peroxidase (TPO), and thyroglobulin (TG) antibodies were all negative. Anti HTLV-I and HIV antibodies were also negative. Thyroid hormone, vitamins, angiotensin-converting enzyme (ACE), and anti-soluble interleukin 2 receptor antibodies were within normal limits. The cerebrospinal fluid (CSF) revealed a leukocyte count of 2 /μL, a protein level of 46.6 mg/dL and a glucose level of 61 mg/dL. IgG index elevated to 0.77 and a polymerase chain reaction for JC virus DNA was negative in the CSF.

A brain CT scan demonstrated diffuse low density in the bilateral cerebral white matter. An MRI disclosed high intensity disseminated throughout the white matter which spread widely from the temporal tip to the pars opercularis (Fig. 1). There was no mass effect or contrast enhancement. On the scout view film of the cervical CT checked 6 months earlier, the low density area in the temporal tip and the frontal white matter was already present.

The background activity of electroencephalography consisted of 8-9 Hz, which suggested moderate dysfunction with left dominance. SPECT showed decreased uptake in accordance with the lesions observed in MRI. Although tocilizumab had been discontinued for the previous 5 months, her cognitive function and MRI findings did not change.

Discussion

The patient developed cognitive impairment in the course of tocilizumab therapy for RA. There are various pathoetiologies which may cause diffuse leukoencephalopathy, including collagen disease, vasculitis, reversible posterior leukoencephalopathy syndrome (RPLS), Binswanger disease, isolated angiitis of the central nervous system (CNS), pro-

gressive multifocal leukoencephalopathy (PML), malignant lymphoma, gliomatosis cerebri, and radiation necrosis (1). The serum autoimmune antibodies examined were all negative and the JC virus DNA in the CSF was negative. The MRI showed asymmetrical white matter lesion and no mass effect, contrast enhancement, or cortical lesions. Thus, we could not obtain any supportive evidence for the diagnosis except the probable relevance with tocilizumab. However, the possibility of infection could not be entirely excluded during the hospitalization; therefore immunological therapy was not given.

Drug-induced leukoencephalopathy has been reported on amphotericin B, acyclovir, methotrexate, fluorouracil, tacrolimus, ciclosporin, etc (2). Also, biological agents, such as etanercept, infliximab, rituximab, or natalizmab cause leukoencephalopathy (3-6). Therefore, we postulated that tocilizumab caused the leukoencephalopathy via immunological mechanisms relating to direct and/or indirect IL-6 signaling. When we consider the concrete mechanism, this patient was aged, hypertensive, and undergoing steroid therapy. These factors might cause a synergistic effect on blood brain barrier (BBB) leading to leukoencephalopathy. Once BBB is disrupted, tocilizumab may also spread to the brain parenchyma and suppress IL-6 related glial survival. In fact, direct injection of IL-6 into the brain can reduce ischemic brain injury, though its mechanism is unknown to date (7).

It remains unknown why the leukoencephalopathy was not resolved after tocilizumab discontinuation. One of the plausible explanations is that the leukoencephalopathy had been so advanced and irreversible that symptomatic relief was not obtained. As mentioned above, because the patient was aged, hypertensive, and undergoing steroid therapy, these backgrounds might have some effects on her irreversible symptoms. The pathological changes might be irreversible demyelination or chronic ischemic changes; however, further study is necessary.

This is the first report regarding the development of leukoencephalopathy during the administration of tocilizumab. Therefore, during tocilizumab therapy, it is strongly recommended to conduct a brain MRI if the patient develops any cognitive impairment.

References

1. Hinchey J, Chaves C, Appignani B, et al. A reversible posterior leukoencephalopathy syndrome. N Engl J Med **334**: 494-500, 1996.
2. Shimono T, Miki Y, Toyoda H, et al. MR imaging with quantitative diffusion mapping of tacrolimus-induced neurotoxicity in organ transplant patients. Eur Radiol **13**: 986-993, 2003.
3. Yamamoto M, Takahashi H, Wakasugi H, et al. Leukoencephalopathy during administration of etanercept for refractory rheumatoid arthritis. Mod Rheumatol **17**: 72-74, 2007.
4. Roos JC. Neurological complication of infliximab. J Rheumatol **34**: 236-237, 2007.
5. US Food and Drug Administration. FDA alert: rituximab (marketed as Rituxan). December 2006.
6. Van Assche G, Van Ranst M, Sciot R, et al. Progressive multifocal leukoencephalopathy after natalizumab therapy for Crohn's disease. N Engl J Med **353**: 362-368, 2005.
7. Suzuki S, Tanaka K, Suzuki N. Ambivalent aspects of interleukin-6 in cerebral ischemia: inflammatory versus neurotrophic aspects. J Cereb Blood Flow Metab **29**: 464-479, 2009.

Neuroscience Research 65 (2009) 263–271

Contents lists available at ScienceDirect

Neuroscience Research

journal homepage: www.elsevier.com/locate/neures

A chemical neurotoxin, MPTP induces Parkinson's disease like phenotype, movement disorders and persistent loss of dopamine neurons in medaka fish

Hideaki Matsui [a,c], Yoshihito Taniguchi [b,c], Haruhisa Inoue [a,c], Kengo Uemura [a,c], Shunichi Takeda [b,c,*], Ryosuke Takahashi [a,c,**]

[a] Department of Neurology, Kyoto University, Graduate School of Medicine, Kyoto 606-8507, Japan
[b] Department of Radiation Genetics, Kyoto University, Graduate School of Medicine, Kyoto 606-8501, Japan
[c] Core Research for Evolutional Science and Technology (CREST), Japan Science and Technology Agency, Japan

ARTICLE INFO

Article history:
Received 16 May 2009
Received in revised form 25 June 2009
Accepted 30 July 2009
Available online 7 August 2009

Keywords:
Parkinson's disease
MPTP
Medaka (*Oryzias latipes*)
Movement disorder
Dopamine
Tyrosine hydroxylase

ABSTRACT

Parkinson's disease (PD) is the second most common neurodegenerative disease associated with the degeneration of dopaminergic neurons in the substantia nigra. To create a new model of PD, we used medaka (*Oryzias latipes*), a small teleost that has been used in genetics and environmental biology. We identified tyrosine hydroxylase (TH) immunopositive dopaminergic and noradrenergic fibers and neurons in the medaka brain. Following establishment of a method for counting the number of dopaminergic neurons and an assay for the evaluation of the medaka behavior, we exposed medaka to 1-methyl-4-phenyl-1,2,3,4-tetrahydropyridine (MPTP). The treatment of medaka at the larval stage, but not at adult stage, decreased the number of dopaminergic cells in the diencephalon and reduced spontaneous movement, which is reminiscent of human PD patients and other MPTP-induced animal PD models. Among TH^+ neurons in the medaka brain, only a specific cluster in the paraventricular area of the middle diencephalon was vulnerable to MPTP toxicity. Detailed examinations of medaka transiently exposed to MPTP at the larval stage revealed that the number of dopaminergic cells was not fully recovered at their adult stage. Moreover, the amounts of dopamine persistently decreased in the brain of these MPTP-treated fish. MPTP-treated medaka is valuable for modeling human PD.

1. Introduction

Parkinson's disease (PD) is characterized by the late-onset degeneration of dopaminergic neurons in a subset of neuronal populations represented by the substantia nigra pars compacta in the midbrain. A small proportion of PD is caused by genetic disorder, which provides invaluable insights into the pathogenesis of sporadic PD (Gasser, 2005). Familial PD is caused by autosomal dominant mutations in the genes encoding *α-synuclein* (Polymeropoulos et al., 1997) and *LRRK2* (Paisán-Ruíz et al., 2004; Zimprich et al., 2004), while juvenile parkinsonism is associated with recessive mutations in the genes encoding *parkin* (Kitada et al., 1998), *DJ-1* (Bonifati et al., 2003), and *PINK1* (Rogaeva et al., 2004; Valente et al., 2004). Various models have been developed in several species in order to understand the mechanisms underlying the pathogenesis of PD, including mouse (Bové et al., 2005; Fleming et al., 2005), *Drosophila* (Cauchi and van den Heuvel, 2006), *Caenorhabditis elegans* (van Ham et al., 2008) and yeasts (Outeiro and Lindquist, 2003). However, the pathogenesis of PD remains largely unknown.

Small laboratory fish such as zebrafish (*Danio rerio*) and Japanese medaka (*Oryzias latipes*) are attractive vertebrate animal models, because they are easy to handle and produce large numbers of progeny per generation (Wittbrodt et al., 2002). Medaka is a small aqueous fish that inhabits Asia and has been used as a model organism since early 1900s (Aida, 1921). It has several advantages over zebrafish or goldfish in modeling PD. First, the whole genome has been sequenced and assembled since the size of medaka genome is only 700 Mb, half the size of the zebrafish genome (Kasahara et al., 2007). Second, several inbred strains have been established in medaka, but not in zebrafish. The lack of genetic variations among individuals may simplify and facilitate genetic studies, and is particularly important for disease models. The goldfish is not suitable for genetic research because it does not have good genetic information nor technology for genetics, while most techniques that are used for zebrafish studies are applicable to medaka. Third, the body of medaka is more transparent than

* Corresponding author at: Department of Radiation Genetics, Kyoto University, Graduate School of Medicine, Yoshida-Konoe-cho, Sakyo-ku, Kyoto 606-8501, Japan. Tel.: +81 75 753 4410; fax: +81 75 753 4419.
** Corresponding author at: Department of Neurology, Kyoto University, Graduate School of Medicine, 54 Shogoin-Kawahara-cho, Sakyo-ku, Kyoto 606-8507, Japan. Tel.: +81 75 751 3770; fax: +81 75 751 9780.
E-mail addresses: stakeda@rg.med.kyoto-u.ac.jp (S. Takeda), ryosuket@kuhp.kyoto-u.ac.jp (R. Takahashi).

0168-0102/$ – see front matter © 2009 Elsevier Ireland Ltd and the Japan Neuroscience Society. All rights reserved.
doi:10.1016/j.neures.2009.07.010

that of the zebrafish or goldfish, and it is easy to visualize the *in vivo* target structures. Fourth, cryopreservation of the sperm is easy and reliable, so we can maintain and store numerous strains in the laboratory (Yang and Tiersch, 2009). Finally and most importantly, we have already retrieved PD-related mutants including *parkin* from our TILLING (Targeting Induced Local Lesions IN Genomes) library of medaka (Taniguchi et al., 2006).

1-Methyl-4-phenyl-1,2,3,4-tetrahydropyridine (MPTP) is a neurotoxin that induces PD-like symptoms. It is metabolized in glial cells to 1-methyl-4-phenylpyridinium (MPP^+), and is subsequently incorporated by dopaminergic neurons via dopamine transporter, thereby selectively damaging the dopaminergic neurons through inhibiting the activity of the mitochondria respiratory chain (Gerlach et al., 1991). It has been widely used to generate zebrafish and goldfish model of PD together with other neurotoxins such as 6-hydroxydopamine and rotenone (Pollard et al., 1992; Anichtchik et al., 2004; Wen et al., 2008; Bretaud et al., 2004; Lam et al., 2005; McKinley et al., 2005). However, these studies mainly focus on the acute or subacute effects of neurotoxins on zebrafish or goldfish. One caveat is that the adult neurogenesis occurs extensively in the brain of fish and that neurons are added continuously to various brain regions (Grandel et al., 2006). Therefore, it is important to examine the consequences of MPTP-induced brain lesions over a long period of time in the research using fish. In this study, we report the long-term effect of MPTP on medaka dopaminergic system evaluated by several assays including histological analysis of dopaminergic neurons and the behavioral tests.

2. Materials and methods

2.1. Fish maintenance

Wild-type medaka of *Kyoto-cab* strain was maintained at 27 °C in a recirculating aquaculture system equipped with carbon filtration, ultraviolet light sterilizers and biofiltration. Adult fish were kept under a reproduction regimen (14 h light/10 h dark). Eggs were kept in a dark box at 28 °C.

2.2. MPTP treatment

The MPTP-hydrochloride (Sigma–Aldrich, MO, USA) was dissolved in distilled water to 10 mg/ml. Safety precautions included the use of protective clothing, globes, goggles, masks and decontamination of all surfaces and solutions with 1% bleach at the end of each experiment. For exposure of adult fish, three fish (90-dpf) were kept in 100 ml of water each containing different concentration of MPTP. The water was changed and MPTP was freshly added to the water every week. Three weeks after treatment, the fish was rinsed seven times for total clearance of MPTP and subjected to the analysis (Fig. 2A). For exposure of larvae, five 10-dpf larvae were kept in a cup containing 50 ml water with various concentration of MPTP. Two days after treatment, MPTP was removed and the fish were used for the analysis (Fig. 2B). We used littermates in a series of experiments and all the experiments were done at least twice.

2.3. High performance liquid chromatography

Brain was homogenized in 100 μl of 0.4 M $HClO_4$ containing 4 mM $Na_2S_2O_5$ and 4 mM diethylenetriaminepentaacetic acid. The supernatant by centrifugation at 18,500 × *g* for 5 min was used for measurement of free catechols. High performance liquid chromatography (HPLC) was conducted with a mobile phase containing bufferA:acetonitrile:methanol = 1000:25.9:62.9 (v/v/v) (bufferA: 0.1 M phosphate, 0.05 M citrate, 4 mM sodium 1-heptanesulfonate and 0.1 mM EDTA, pH 3.0). Dopamine and metabolites were detected with series coulometric detector (ESA, Inc., Chelmsford, MA, USA). Data were collected and processed on a CHROMELEON™ Chromatography Data Systems 6.40 (Dionex, Sunnyvale, CA, USA). The pellet was then reserved for the analysis of the protein content. For this purpose, the pellet was solubilized in 100 μl of 0.5 N NaOH at 60 °C and the protein was quantified by the BCA assay method, using bovine serum albumin (BSA) as the standard.

2.4. Immunohistochemistry

After organs were examined under the stereomicroscope, fish were fixed in 4% paraformaldehyde for 24 h and embedded in paraffin. Each brain was sectioned at 20-μm thickness and incubated with mouse anti-tyrosine hydroxylase (TH) antibody (Millipore, MA, USA, 1:500) for 1 h. Immunoperoxidase detection was carried out by using Vector Elite ABC kit with DAB (Vector Laboratories, CA, USA) on every section. The number of dopaminergic neurons in the diencephalon was determined by counting the nucleus of TH^+ neurons in coronal sections using OLYMPUS BX51 microscope with MICROFIRE digital camera (Olympus, Japan) and Stereo Investigator (MBF Bioscience, VT, USA). Photographs were taken by the same equipments. Whole mount immunohistochemistry of larvae was carried out as previously described (Shimamura and Takeichi, 1992). Mouse anti-TH antibody (Millipore, MA, USA, 1:100) was detected via fluorescence using anti-mouse IgG conjugated with Alexa Fluor 546 (Invitrogen, WI, USA). Images were acquired by LSM510 microscope (Carl Zeiss, Germany) and subjected to quantitative analysis using Photoshop (Adobe, CA, USA).

2.5. Western blotting

Brains were homogenized in RIPA buffer (25 mM Tris–HCl pH 7.6, 150 mM NaCl, 1% NP-40, 1% sodium deoxycholate, 0.1% SDS) with protease inhibitors and processed for SDS-PAGE. Immunoreactive bands were detected with ECL reagent or ECL plus reagent (GE Healthcare Life Sciences, Japan) and chemiluminescent signal was visualized by the exposing membrane to Fuji RX-U X-ray film (Fuji Film, Japan). Films were scanned and densitometric analysis of blots was performed using ImageJ software (National Institute of Health). The background intensity of the film was subtracted from the band intensity. Anti-TH monoclonal antibody (1:1000, mouse anti-TH, MAB318, Millipore) was used for the western blotting analysis of TH. For the loading control, anti-β-actin monoclonal antibody (1:5000, AC-15, Sigma–Aldrich) was used.

2.6. Behavioral analysis

Fish were subjected to a spontaneous swimming measuring test during a light phase. Images were collected by a video camera positioned above the water tank under a low indirect dimly white light, and analyzed by a computer-assisted system (Muromachi Kikai, Japan). The water tank was a transparent circular field (2 cm water depth, 27 °C) with the diameter of 5 cm for larvae and 20 cm for adults. We started to acquire the images 1 min after the larvae was entered into the water tank. Adult medaka is more wary of environmental changes compared to zebrafish and larval medaka, and they tend to remain stationary when put in a new tank. We started to acquire the images 1 min after the adult fish began to move in a new water tank. Beginning of this movement was automatically defined when fish moved from one section to another section (Fig. 5D). The data were collected for 1 or 5 min for larvae and adults, respectively. The larvae and adults were judged as they were swimming only when the moving speed exceeded 0.025 cm/0.1 s and 0.1 cm/0.1 s, respectively. Total swimming distance, frequency of swimming movement (duration of swimming movement divided by the total time of observation), and swimming velocity (total swimming distance divided by duration of swimming movement) were measured and compared among the groups.

2.7. Statistical analysis

Data were expressed as mean ± standard error of the mean (SEM). The results were statistically evaluated for significance by applying ANOVA with post hoc analysis using Dunnett's test. Differences were considered significant when $p < 0.05$.

3. Results

3.1. Distribution of dopaminergic neurons in the brain of adult medaka

To examine the distribution of dopaminergic neurons in medaka brain, we used immunohistochemistry of TH to visualize dopaminergic neurons. We identified TH immunopositive (TH^+) fibers in the telencephalon (Fig. 1B). This TH^+ structure in the teleost brain is relevant to the striatum in the human brain (Rink and Wullimann, 2004). Medaka TH^+ neurons aligned from the telencephalon to the diencephalon along the ventro-medial side of the brain (Fig. 1C–F). In the rostral part of diencephalon, clusters of small neurons were found in both dorsal and ventral areas (Fig. 1D). Large TH^+ neurons were distributed towards the caudal area around the ventricle in the middle diencephalon (Fig. 1E). The rostro-ventral TH cluster was around the nucleus posterioris periventricularis (NPPv) and the middle one around the NPPv and the nucleus anterior tuberis. At the most caudal part of the diencephalon, there were small neurons on the dorsal side (Fig. 1F). This cluster existed around the nucleus posterior thalami. We could easily distinguish these clusters because the size of neurons

in each cluster was different and these clusters were clearly separated anatomically from each other. We also detected TH^+ noradrenergic neurons in the medulla oblongata (Fig. 1G).

The distribution of TH^+ neurons in the medaka diencephalon largely matched with previously published data on zebrafish TH^+ neurons and medaka neurons that exhibit *Nurr1* mRNA (Rink and Wullimann, 2004; Kapsimali et al., 2001). Histological examination using retrograde tracers suggests that a subset of dopaminergic neurons in the diencephalon of zebrafish project to the striatum-like structure and may be equivalents of the substantia nigra neurons in mammals (Rink and Wullimann, 2004). For the subsequent experiments in this study, we counted only the number of dopaminergic neurons in the diencephalic clusters because these will contain an equivalent of the substantia nigra. TH^+ neurons in the middle diencephalon show a distinct morphology with the large cell body and the intense cytoplasmic staining hollowed by a clear nucleus (Supplementary Fig. 1). There are 87.5 ± 5.6 ($n = 8$) of such cells in around 200 μm in the paraventriclular area of the middle diencephalon (Fig. 3C). In the rostral and caudal regions to this area, we found 145.9 ± 9.1 and 81.9 ± 8.0 TH^+ neurons, respectively, with a smaller cell body (Fig. 3C). Counting these cells yielded highly reproducible data. We also counted the number of TH^+ neurons

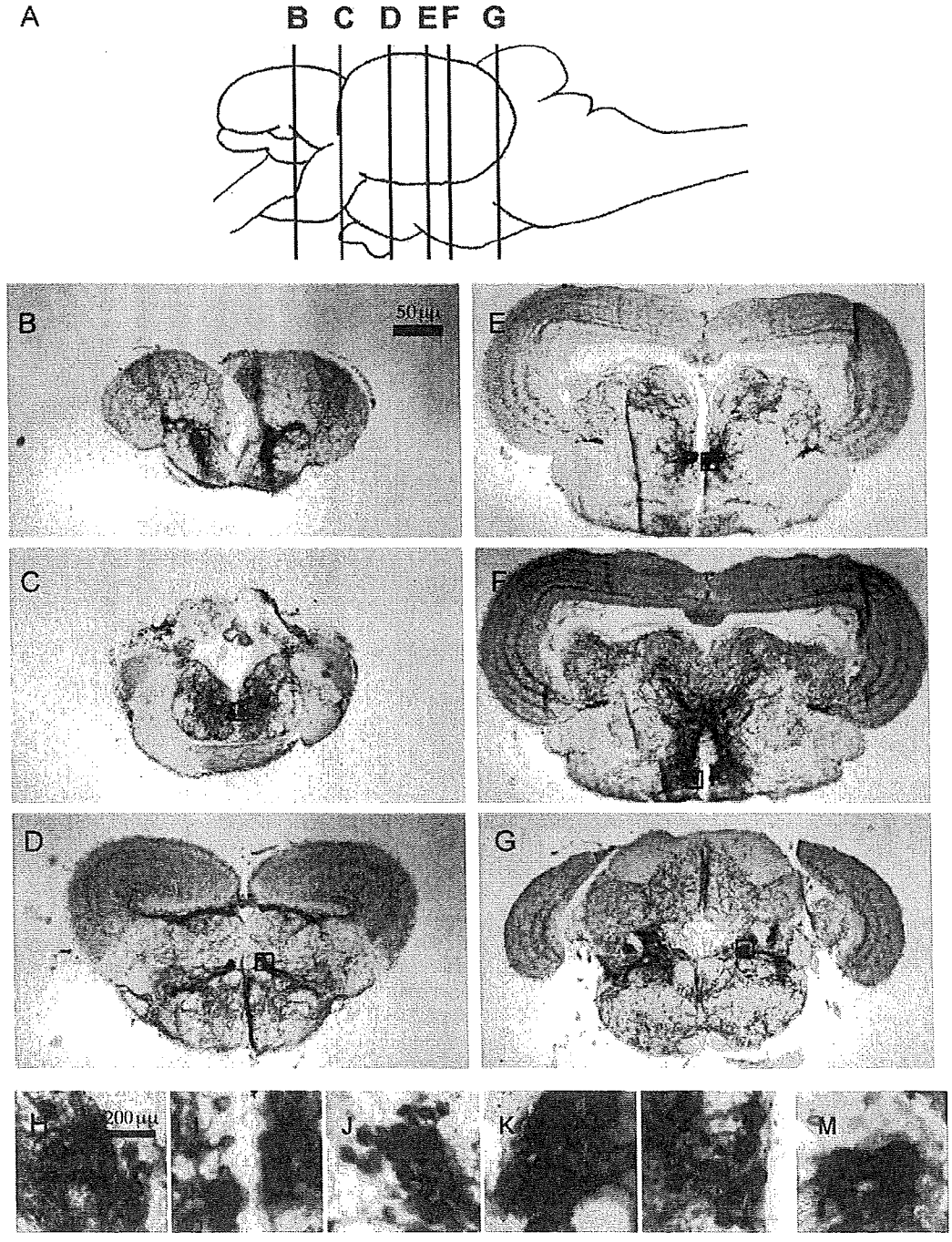

Fig. 1. The distribution of TH^+ neurons in adult medaka diencephalon and medulla oblongata. Coronal sections at different rostro-caudal levels show the localization of TH^+ dopaminergic fibers and neurons in the telencephalon (B), preoptic area (C) and diencephalon (D: rostral, E: middle, F: caudal). TH^+ neurons were also distributed in the medulla oblongata (G). Insets (H–M) are the magnified picture of original images (B–G) respectively. The positions of each section are illustrated by vertical lines in (A).

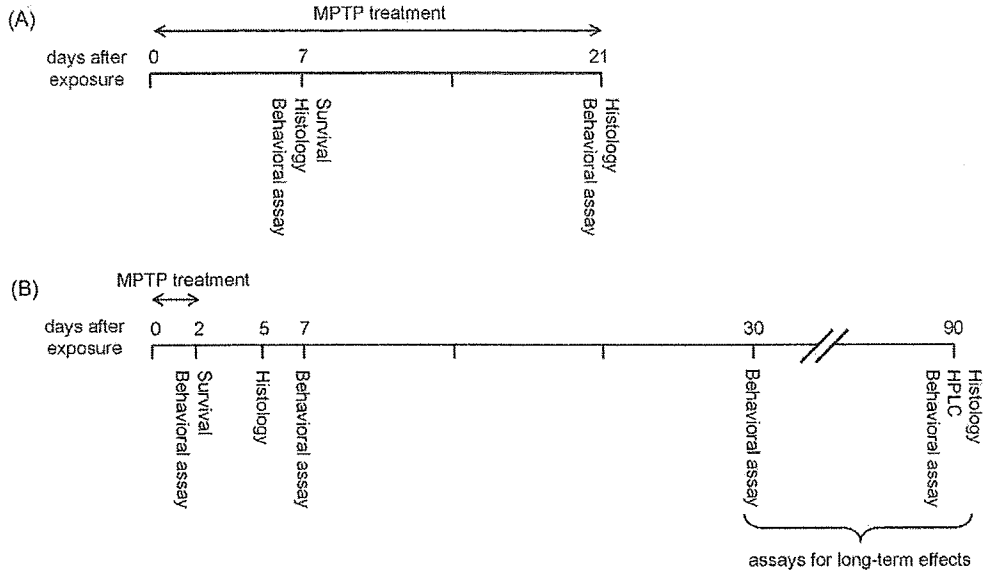

Fig. 2. MPTP treatment schedule. (A) For 3 weeks exposure to adult fish. 90-dpf fish were exposed to MPTP. MPTP was removed 21 days after the first exposure (111-dpf) and the brains of these fish were immediately fixed for histology. (B) For 2 days exposure to larvae. 10-dpf fish were exposed to MPTP. MPTP was removed 2 days after the first exposure (12-dpf). Assays including HPLC, behavioral analysis and histology were done at the indicated time course. The numbers indicate the days after the first exposure to MPTP.

(43.8 ± 4.2) in the medulla oblongata to monitor the effect of MPTP on noradrenergic neurons. In summary, we identified several clusters of TH^+ neurons in medaka brain and established a reliable method for evaluating the number of dopaminergic neurons.

3.2. Short-term effect of MPTP on adult and larval medaka

Several studies have been reported regarding the cytotoxic effect of MPTP on zebrafish and goldfish. In order to investigate the interspecies differences of sensitivity to MPTP between medaka and other model teleost fish, we treated 3 months old and 10-dpf (days post-fertilization) medaka with varying concentration of MPTP for 1 week (Fig. 2A). The embryonic development is slow in medaka in comparison to zebrafish, and it usually takes 7–10 days for medaka larvae before hatching out of the eggshell.

When the adult fish were exposed to 0.1 μg/ml of MPTP, all the fish (10 out of 10) survived a-week-long treatment, whereas 0.2 μg/ml of MPTP was tolerated by only a small fraction of fish (2

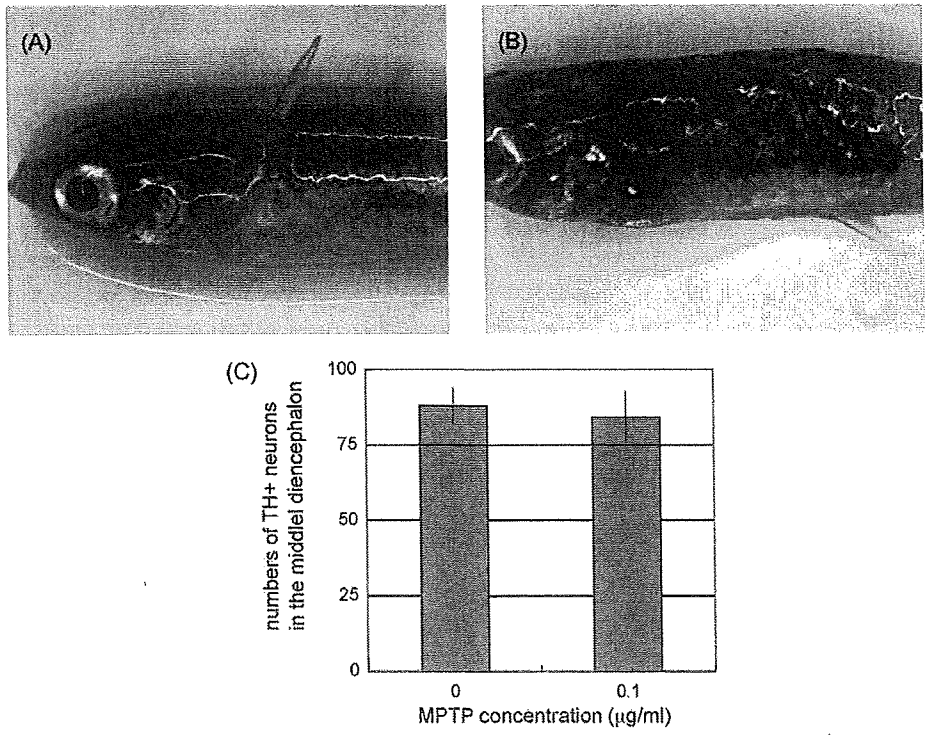

Fig. 3. Features of fish exposed to MPTP at the adult stage. (A and B) Skin images of control fish (A) and MPTP-treated fish (B). The skin was darkened by MPTP treatment (white allow). (C) The numbers of TH^+ neurons in the middle diencephalon. There was no significant reduction in the TH^+ neurons of MPTP-treated fish. $n = 8$ for each group.

out of 10). Following the treatment with 0.1 μg/ml of MPTP, the skin became darkly pigmented as in the MPTP-treated zebrafish (Fig. 3A and B), presumably due to the impairment of peripheral catecholaminergic nerves (Bretaud et al., 2004). However there was no significant decrease in the number of TH^+ cells in the diencephalon and medulla oblongata, nor in the level of spontaneous swimming movement of the MPTP-treated adult medaka at 0.1 μg/ml (data not shown). Prolonged exposure of up to 3 weeks also did not alter the number of TH^+ neurons nor the spontaneous movement (Fig. 3C, data not shown).

Next, we sought to determine the effect of MPTP on medaka larvae since higher sensitivity of TH^+ neurons to MPTP has been reported in zebrafish larvae compared to the adult (McKinley et al., 2005). When medaka larvae were treated with 0.2 μg/ml of MPTP for 2 days, 35 out of 50 (70%) fish survived, while only 1 out 10 (10%) survived after the treatment with 0.3 μg/ml of MPTP. The cytotoxic effect of MPTP on dopaminergic neurons in larvae was then determined by the whole mount immunohistochemistry 3 days after the end of exposure to 0.2 μg/ml of MPTP. In contrast to the fish exposed to MPTP at the adult stage, the TH^+ signal in the diencephalon was markedly decreased in the fish exposed to MPTP at the larval stage (Fig. 4C). The quantitative analysis showed 84% decrease in the TH^+ signal in the MPTP-treated fish compared to the non-treated control (Fig. 4E). These results indicate that the MPTP elicits the reduction of TH^+ neurons in medaka larvae, but not in the adult fish.

Since the histological analysis showed that MPTP impaired dopaminergic neurons, we monitored the spontaneous swimming movement of larvae exposed to 0.2 μg/ml of MPTP using the automated tracking system. Starting immediately after the end of exposure, MPTP-treated fish showed marked decrease in the total swimming distance (Fig. 5A). Additionally, the MPTP treatment significantly diminished the frequency and velocity of swimming (Fig. 5B and C). Although 0.2 μg/ml of MPTP is much lower than the concentration used in previous reports in zebrafish (5–45 μg/ml) (McKinley et al., 2005; Wen et al., 2008; Bretaud et al., 2004), even lower concentration of MPTP (0.02 μg/ml) showed the reduction in both the number of TH^+ neurons and the spontaneous movement (Fig. 5A–D). The group treated with 0.02 μg/ml of MPTP exhibited the intermediate phenotype between the control and the group treated with 0.2 μg/ml of MPTP, suggesting the dose–response relationship. To exclude the possibility of symptoms other than PD, we forced the fish to swim by giving them a touch or sound stimulus. We found that MPTP-treated fish and their untreated controls displayed comparable quick response to these stimuli (data not shown), suggesting that MPTP affects the spontaneous movement of medaka without associating with muscle weakness, paralysis and sensory defect.

3.3. *Persistent loss of dopaminergic neurons in the brain of medaka exposed to MPTP at the larval stage*

Not a few studies have revealed the cytotoxic effect of MPTP on TH^+ cells in teleost fish (Pollard et al., 1992; Anichtchik et al., 2004; Wen et al., 2008; Bretaud et al., 2004; Lam et al., 2005; McKinley

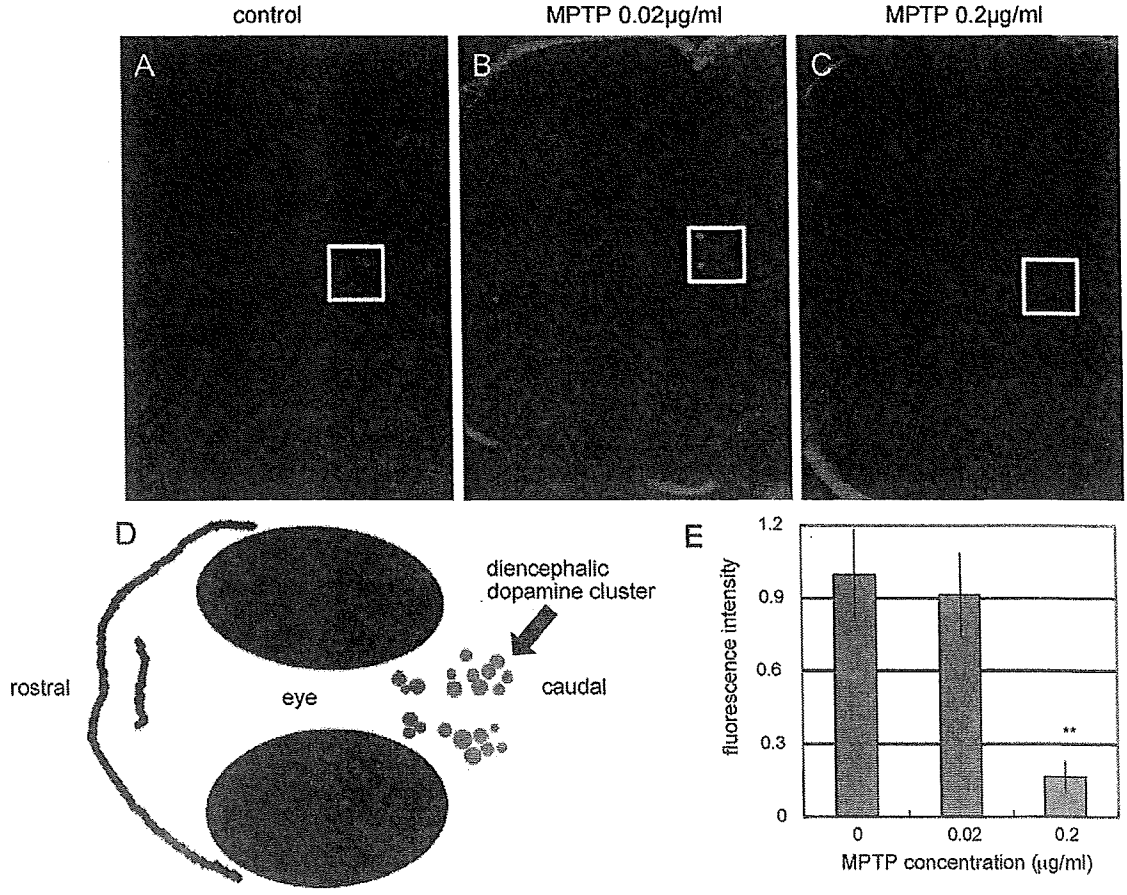

Fig. 4. Whole mount TH staining of medaka larvae following exposure to MPTP. White squares indicated diencephalic dopamine neurons. Images were taken 5 days after the first exposure (15-dpf) (A: control, B: MPTP 0.02 μg/ml and C: MPTP 0.2 μg/ml), and were used quantitative analysis. (D) Showed simple atlas of the images. (E) Quantitative comparisons of the fluorescence of TH^+ neurons. The region of interest was set as a minimal square including TH^+ neurons in the diencephalon. 0.2 μg/ml MPTP treatment markedly reduced TH^+ signals in the diencephalon (C and E). $^{**}p < 0.01$ vs. control. $n = 4$ for each group.

et al., 2005). However, it is important to investigate the long-term effect of MPTP-induced depletion of dopaminergic neurons because it has been known that the fish has a strong regenerative capacity of the brain structures (Zupanc, 2008). To this end, we exposed 10-dpf larvae to 0.2 μg/ml MPTP for 2 days, and measured the amounts of both dopamine and 3,4-dihydroxyphenylacetic acid (DOPAC), a metabolite of dopamine, in the whole brain at 3 months after the MPTP treatment. We verified that both dopamine and DOPAC of the whole brain significantly decreased in MPTP-treated fish in comparison with non-treated control fish (Fig. 6A and B). DOPAC/dopamine ration was increased significantly and this was consistent with other MPTP models (Fig. 6D) (Irwin et al., 1990). The reduction of dopamine and DOPAC may not reflect general toxicity of MPTP towards the whole neurons, because MPTP did not diminish the level of norepinephrine (Fig. 6C).

To confirm whether MPTP injured the cluster of the diencephalic TH^+ neurons, leading to the decline of dopamine content in the brain, we counted the number of TH^+ cells in the brain. The number of TH^+ dopaminergic neurons in the middle diencephalon was significantly less in the MPTP-treated group than that in the non-treated control group (Fig. 7A–C). In contrast to the dopaminergic neurons in the middle diencephalon, the TH^+ signal intensity of dopaminergic fibers in the telencephalon were scarcely affected by MPTP possibly reflecting the recovery of these fibers after MPTP exposure at their larval stage (data not shown). The number of TH^+ neurons in the rostro-ventral and the caudal part of the diencephalon, and in the medulla oblongata also did not show statistically significant differences (Fig. 7C). Western blot analysis of whole brain extract disclosed a slight, albeit not statistically significant, decrease in the level of TH protein in the MPTP-treated groups (Fig. 7D). These data suggest that MPTP imposed on the

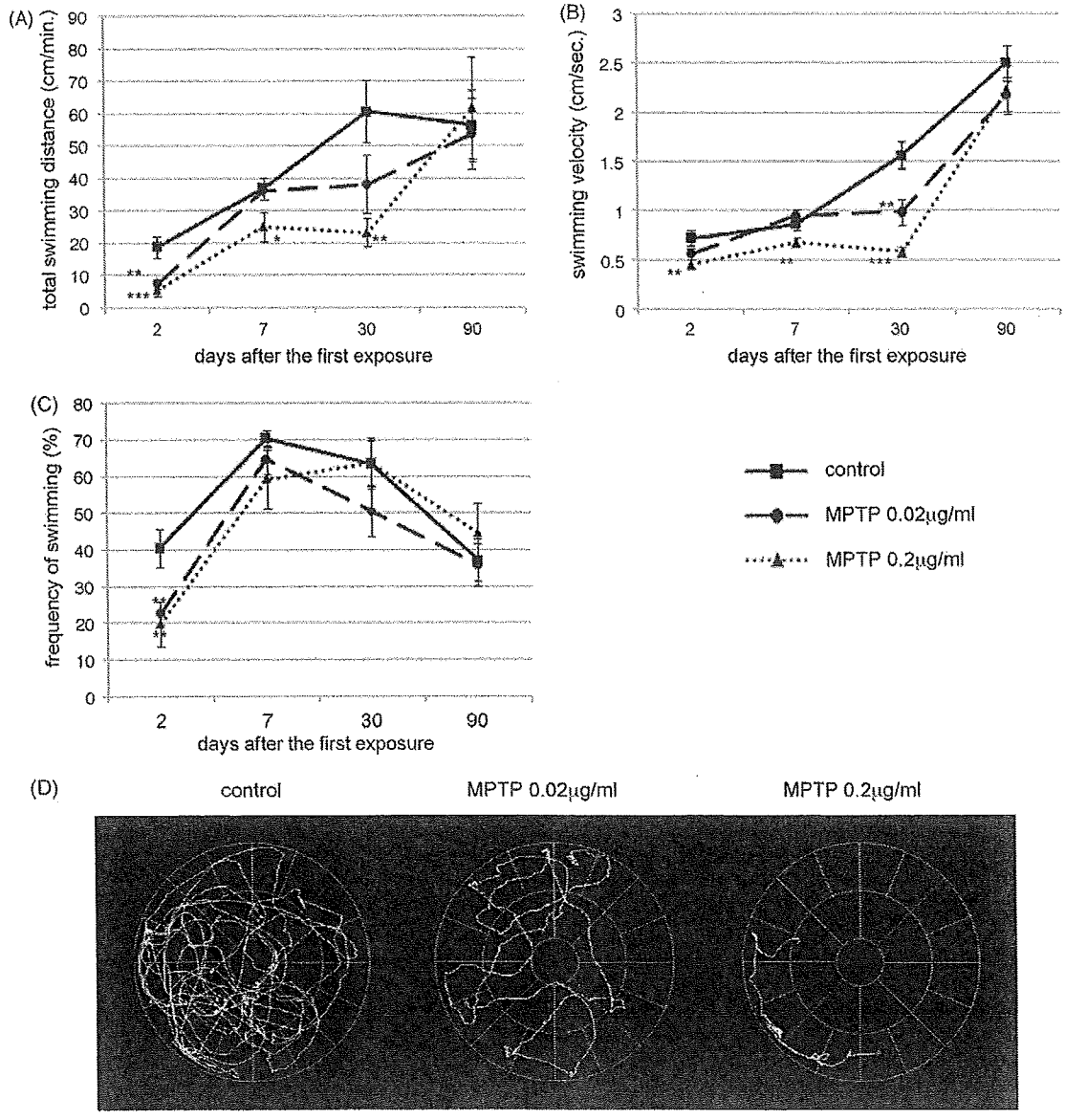

Fig. 5. Spontaneous movement analysis of MPTP-treated medaka. (A) Total swimming distance (cm/min), (B) swimming velocity (cm/s), (C) frequency of swimming movement (%), (D) representative swimming track immediately after the 2 days exposure of MPTP. Total swimming distance and swimming velocity of 0.2 μg/ml MPTP-treated fish decreased significantly 2, 7 and 30 days after the first exposure (12, 17 and 40-dpf) (A, B and D). The frequency of swimming movement also decreased 2 days after the first exposure (12-dpf) (C). The MPTP-treated fish showed gradual recovery from the defective movement and all the parameters did not differ among the groups 90 days after the first exposure (100-dpf) (A–C). $^*p < 0.05$, $^{**}p < 0.01$, $^{***}p < 0.001$ vs. control. $n = 10$ for each group.

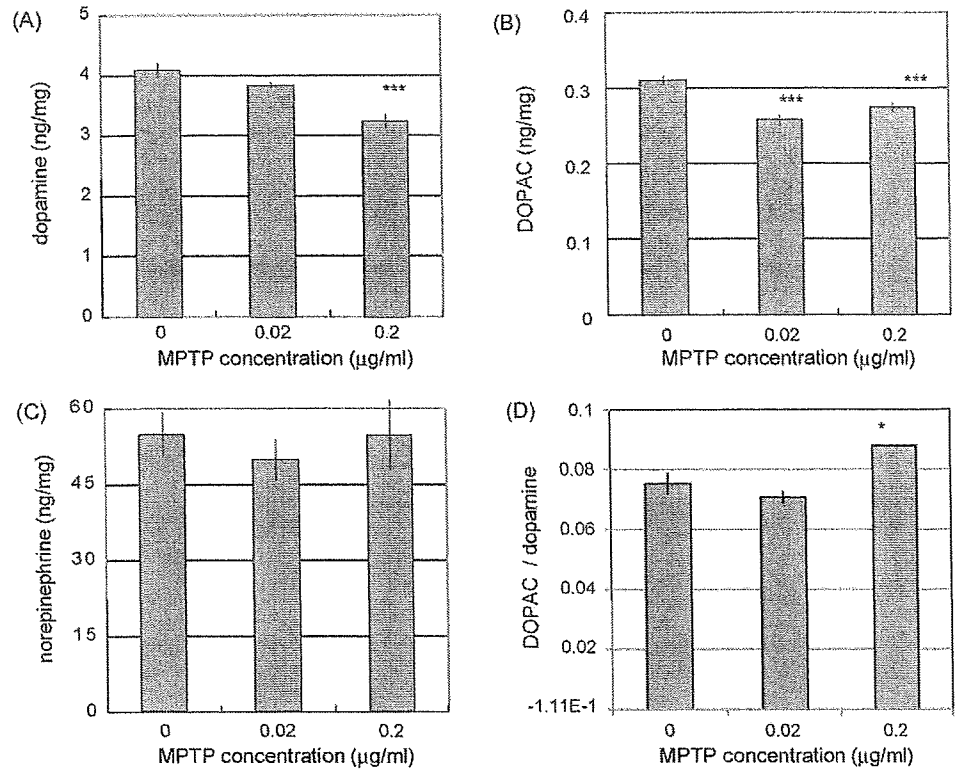

Fig. 6. HPLC analysis of neuro-transmitters in MPTP-treated medaka. Dopamine (A), DOPAC (B) and norepinephrine (C) amount in the whole brain of adult (100-dpf) medaka treated with water (control), 0.02 μg/ml MPTP and 0.2 μg/ml MPTP at the larval stage. All values are presented as the amount (ng) per protein weight (mg). Dopamine and DOPAC were decreased in 0.2 μg/ml MPTP-treated fish (A and B). Norepinephrine did not differ among the groups (C). (D) Showed DOPAC/dopamine ratio. $^{*}p < 0.05$, $^{***}p < 0.001$ vs. control. $n = 8$ for each group.

larval stage causes selective and persistent loss of the middle diencephalic TH^+ neurons after 3 months of exposure.

Next, we investigated a long-term effect of MPTP on neurological function by monitoring the spontaneous swimming movement of medaka over time. One month after the exposure, the frequency of swimming movement in MPTP-treated group completely recovered to the level of non-treated fish (Fig. 5C), although the total swimming distance and the velocity of swimming still decreased in MPTP-treated group (Fig. 5A and B). Three months after the exposure, the MPTP-treated group displayed the complete recovery of all the parameters of swimming movement tested (Fig. 5A–C). In summary, although MPTP treatment at the larval stage may irreversibly damage specific cluster of diencephalic TH^+ neurons and thereby decrease the amount of dopamine in the whole brain, the suppressive effect of MPTP on the spontaneous movement is observed only transiently and disappears 3 months after the exposure to MPTP.

4. Discussion

We here identified TH^+ dopaminergic neurons and noradrenergic neurons in the medaka brain. The larvae exposed to MPTP showed dopaminergic cell loss and reduced spontaneous movement. When these fish reached to an adult stage, they still displayed the loss of dopaminergic neurons associated with reduced amounts of dopamine in the whole brain, although the movement deficit gradually recovered to the normal level. Remarkably, MPTP-induced neuronal loss was restricted to the middle diencephalic clusters, which may include substantia nigra-like structure in teleosts. Therefore, we reasoned that the MPTP treatment at the larval stage allows the establishment of a medaka model of PD.

We demonstrated the specific toxicity of MPTP towards TH^+ neurons in the middle diencephalon. Other TH^+ neurons including diencephalic neurons outside this region and the neurons in medulla oblongata did not show the reduction in number. The vulnerability of the neurons in the paraventricular area of the middle diencephalon to MPTP, together with their anatomical features, supports the idea that these cells are the bona fide an equivalent of the substantia nigra in mammals. Toxic effect of MPTP specific to diencephalic TH^+ neurons was also reported in zebrafish (McKinley et al., 2005; Wen et al., 2008; Bretaud et al., 2004). By contrast, several other reports showed the reduction of not only dopaminergic but also norepinephrinergic neurons in MPTP-treated zebrafish and goldfish (Pollard et al., 1992; Anichtchik et al., 2004). The differential toxic effects of MPTP on norepinephrinergic neurons may depend on the routes of drug administration, as we noticed that in these reports the injection of MPTP into adult fish led to the injury of norepinephrinergic neurons, whereas submerging the fish in the water containing MPTP affected only dopaminergic neurons. We speculate that the pharmacodynamics is quite different between these two methods, with injection leading to a very high concentration in various tissues. Recent report showed the broad toxicity of MPTP not only on dopaminergic neurons but also on noradrenergic and histaminergic neurons even though they exposed zebrafish to the water containing MPTP (Sallinen et al., 2009). Because the amount of MPTP they used is much higher than our report, we speculate that this may be due to the broader spectrum injury of MPTP.

It is also an intriguing question whether the peripheral tissue is damaged by MPP^+ generated by peripheral MAO-B as suggested by MPTP-induced skin color change (Fig. 3A and B). The metabolic pathway and distribution of MPTP and MPP^+ in medaka should be investigated in the future.

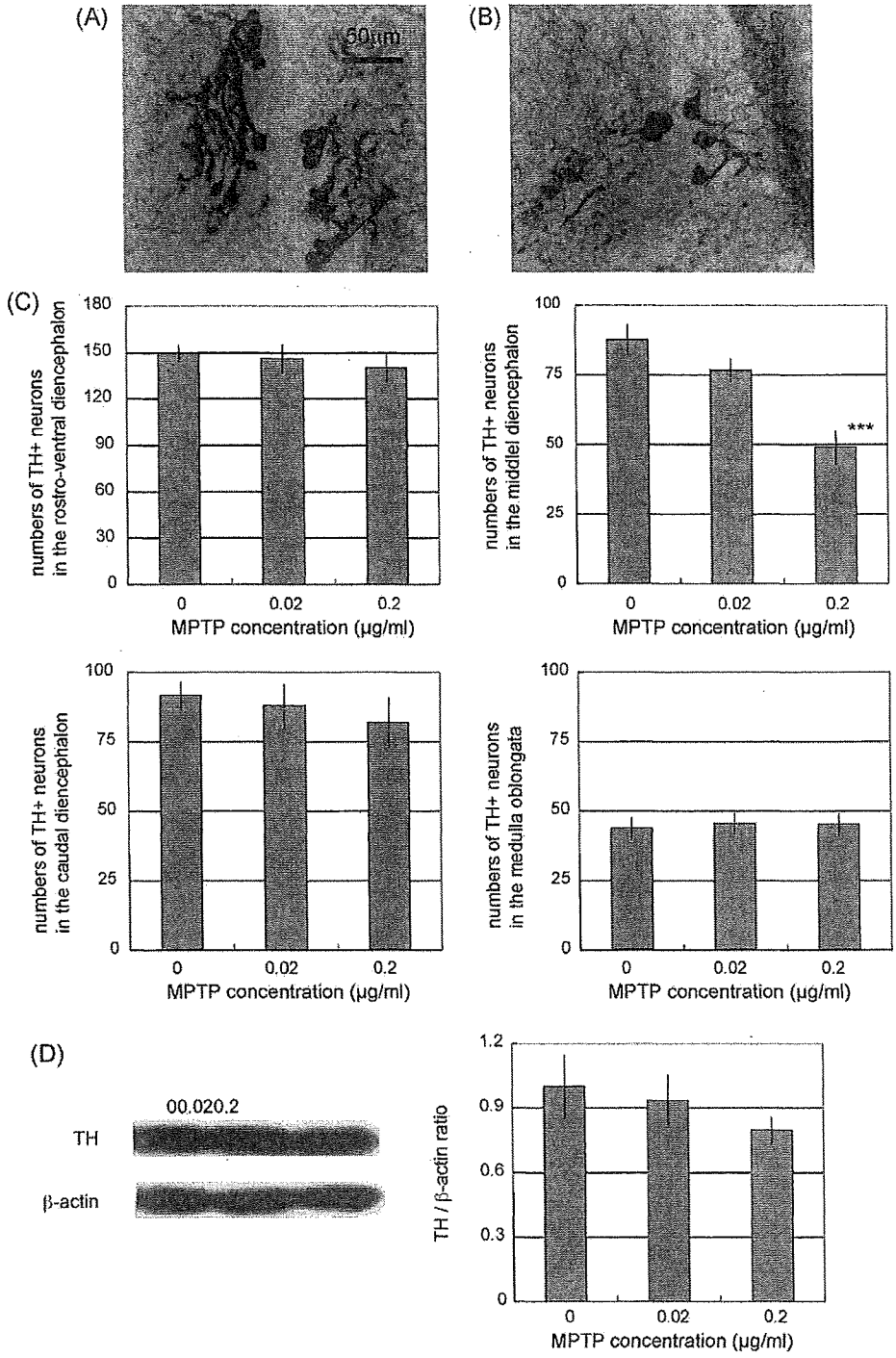

Fig. 7. TH immunohistochemistry and western blotting of adult medaka treated with MPTP at their larval stage. Samples were fixed 90 days after the first exposure (100-dpf). Coronal sections taken from the diencephalon level showed TH^+ neurons in control fish (A) and 0.2 μg/ml MPTP-treated fish (B). The numbers of TH^+ neurons in the middle diencephalon decreased significantly in MPTP-treated medaka (C). The numbers of TH^+ neurons in the rostro-ventral and caudal diencephalon, and the medulla oblongata did not show significant differences (C). $^{***}p < 0.001$ vs. control. $n = 8$ for each group. (D) The protein amount of TH in the whole brain of the control, 0.02 μg/ml MPTP-treated and 0.2 μg/ml MPTP-treated fish is examined by western blotting and then normalized by β-actin (loading control). The graph shows the ratio of TH/β-actin amount in each genotype (the average amount of control fish = 1). The amount of TH protein did not differ significantly among the groups. $n = 4$ for each group.

Previous studies of zebrafish and goldfish did not follow the long time course of MPTP toxicity, but continuous observation is important for the model animal because of the following reasons. First, PD is a late-onset and long-lasting neurodegenerative disorder. Second, the brains of teleost fish show widespread adult neurogenesis and new TH^+ cells are added in the olfactory bulb and diencephalon (Grandel et al., 2006). We here show the gradual functional recovery of dopaminergic neurons in the fish transiently exposed to MPTP at the larval stage, as evidenced by increases in spontaneous movement. Such behavioral recovery has been reported in several mammalian species after MPTP treatment (Rose et al., 1989; Elsworth et al., 1990, 2000; Kurlan et al., 1991).

The degree of the recovery is variable and may be dependent on several factors, including the protocol of MPTP treatment, the species, and the method of behavioral evaluation. Interestingly, the functional recovery observed in medaka was not accompanied by the restoration of the number of TH^+ cells or by increase in the amount of dopamine to a normal level in the adult stage. The striatum of MPTP-treated medaka did not show robust denervation of the TH^+ neurons, and this may explain the behavioral recovery observed in our medaka. Such complete behavioral recovery despite the incomplete return of the amount of dopamine may take place as in squirrel monkeys, possibly due to alteration in dopamine metabolism and neuronal sprouting (Petzinger et al., 2006).

In summary we have generated a medaka PD model by treating larval fish with MPTP, and established reliable assays from the larval stage to the adult. Our protocol of inducing PD-like phenotypes and our assay described in this study provides invaluable tools to investigate medaka model of familial PD retrieved from the TILLING library or medaka treated by other toxins or drugs.

Acknowledgements

We are grateful to all the technical staff of the Department of Radiation Genetics and all the people of the Department of Neurology.

Appendix A. Supplementary data

Supplementary data associated with this article can be found, in the online version, at doi:10.1016/j.neures.2009.07.010.

References

Aida, T., 1921. On the inheritance of color in a fresh-water fish, *Aplocheilus latipes* Temminck and Schlegel, with special reference to sex-linked inheritance. Genetics 6, 554–573.

Anichtchik, O.V., Kaslin, J., Peitsaro, N., Scheinin, M., Panula, P., 2004. Neurochemical and behavioral changes in zebrafish *Danio rerio* after systemic administration of 6-hydroxydopamine and 1-methyl-4-phenyl-1,2,3,6-tetrahydropyridine. J. Neurochem. 88, 443–453.

Bonifati, V., Rizzu, P., van Baren, M.J., Schaap, O., Breedveld, G.J., Krieger, E., Dekker, M.C., Squitieri, F., Ibanez, P., Joosse, M., van Dongen, J.W., Vanacore, N., van Swieten, J.C., Brice, A., Meco, G., van Duijn, C.M., Oostra, B.A., Heutink, P., 2003. Mutations in the DJ-1 gene associated with autosomal recessive early-onset parkinsonism. Science 299, 256–259.

Bové, J., Prou, D., Perier, C., Przedborski, S., 2005. Toxin-induced models of Parkinson's disease. NeuroRx 2, 484–494.

Bretaud, S., Lee, S., Guo, S., 2004. Sensitivity of zebrafish to environmental toxins implicated in Parkinson's disease. Neurotoxicol. Teratol. 26, 857–864.

Cauchi, R.J., van den Heuvel, M., 2006. The fly as a model for neurodegenerative diseases: is it worth the jump? Neurodegener. Dis. 3, 338–356.

Elsworth, J.D., Deutch, A.Y., Redmond Jr., D.E., Sladek Jr., J.R., Roth, R.H., 1990. MPTP-induced parkinsonism: relative changes in dopamine concentration in subregions of substantia nigra, ventral tegmental area and retrorubral field of symptomatic and asymptomatic vervet monkeys. Brain Res. 513, 320–324.

Elsworth, J.D., Taylor, J.R., Sladek Jr., J.R., Collier, T.J., Redmond Jr., D.E., Roth, R.H., 2000. Striatal dopaminergic correlates of stable parkinsonism and degree of recovery in old-world primates one year after MPTP treatment. Neuroscience 95, 399–408.

Fleming, S.M., Fernagut, P.O., Chesselet, M.F., 2005. Genetic mouse models of parkinsonism: strengths and limitations. NeuroRx 2, 495–503.

Gasser, T., 2005. Genetics of Parkinson's disease. Curr. Opin. Neurol. 18, 363–369.

Gerlach, M., Riederer, P., Przuntek, H., Youdim, M.B., 1991. MPTP mechanisms of neurotoxicity and their implications for Parkinson's disease. Eur. J. Pharmacol. 208, 273–286.

Grandel, H., Kaslin, J., Ganz, J., Wenzel, I., Brand, M., 2006. Neural stem cells and neurogenesis in the adult zebrafish brain: origin, proliferation dynamics, migration and cell fate. Dev. Biol. 295, 263–277.

Irwin, I., DeLanney, L.E., Forno, L.S., Finnegan, K.T., Di Monte, D.A., Langston, J.W., 1990. The evolution of nigrostriatal neurochemical changes in the MPTP-treated squirrel monkey. Brain Res. 531, 242–252.

Kapsimali, M., Bourrat, F., Vernier, P., 2001. Distribution of the orphan nuclear receptor Nurr1 in medaka (*Oryzias latipes*): cues to the definition of homologous cell groups in the vertebrate brain. J. Comp. Neurol. 431, 276–292.

Kasahara, M., Naruse, K., Sasaki, S., Nakatani, Y., Qu, W., Ahsan, B., Yamada, T., Nagayasu, Y., Doi, K., Kasai, Y., Jindo, T., Kobayashi, D., Shimada, A., Toyoda, A., Kuroki, Y., Fujiyama, A., Sasaki, T., Shimizu, A., Asakawa, S., Shimizu, N., Hashimoto, S., Yang, J., Lee, Y., Matsushima, K., Sugano, S., Sakaizumi, M., Narita, T., Ohishi, K., Haga, S., Ohta, F., Nomoto, H., Nogata, K., Morishita, T., Endo, T., Shin-I, T., Takeda, H., Morishita, S., Kohara, Y., 2007. The medaka draft genome and insights into vertebrate genome evolution. Nature 447, 714–719.

Kitada, T., Asakawa, S., Hattori, N., Matsumine, H., Yamamura, Y., Minoshima, S., Yokochi, M., Mizuno, Y., Shimizu, N., 1998. Mutations in the parkin gene cause autosomal recessive juvenile parkinsonism. Nature 392, 605–608.

Kurlan, R., Kim, M.H., Gash, D., 1991. The time course and magnitude of spontaneous recovery of parkinsonism produced by intracarotid administration of 1-methyl-4-phenyl-1,2,3,6-tetrahydropyridine to monkeys. Ann. Neurol. 29, 677–679.

Lam, C.S., Korzh, V., Strahle, U., 2005. Zebrafish embryos are susceptible to the dopaminergic neurotoxin MPTP. Eur. J. Neurosci. 21, 1758–1762.

McKinley, E.T., Baranowski, T.C., Blavo, D.O., Cato, C., Doan, T.N., Rubinstein, A.L., 2005. Neuroprotection of MPTP-induced toxicity in zebrafish dopaminergic neurons. Brain Res. Mol. Brain Res. 141, 128–137.

Outeiro, T.F., Lindquist, S., 2003. Yeast cells provide insight into alpha-synuclein biology and pathobiology. Science 302, 1772–1775.

Paisán-Ruíz, C., Jain, S., Evans, E.W., Gilks, W.P., Simón, J., van der Brug, M., López de Munain, A., Aparicio, S., Gil, A.M., Khan, N., Johnson, J., Martinez, J.R., Nicholl, D., Carrera, I.M., Pena, A.S., de Silva, R., Lees, A., Martí-Massó, J.F., Pérez-Tur, J., Wood, N.W., Singleton, A.B., 2004. Cloning of the gene containing mutations that cause PARK8-linked Parkinson's disease. Neuron 44, 595–600.

Petzinger, G.M., Fisher, B., Hogg, E., Abernathy, A., Arevalo, P., Nixon, K., Jakowec, M.W., 2006. Behavioral motor recovery in the 1-methyl-4-phenyl-1,2,3,6-tetrahydropyridine-lesioned squirrel monkey (*Saimiri sciureus*): changes in striatal dopamine and expression of tyrosine hydroxylase and dopamine transporter proteins. J. Neurosci. Res. 83, 332–347.

Pollard, H.B., Dhariwal, K., Adeyemo, O.M., Markey, C.J., Caohuy, H., Levine, M., Markey, S., Youdim, M.B., 1992. A parkinsonian syndrome induced in the goldfish by the neurotoxin MPTP. FASEB J. 6, 3108–3116.

Polymeropoulos, M.H., Lavedan, C., Leroy, E., Ide, S.E., Dehejia, A., Dutra, A., Pike, B., Root, H., Rubenstein, J., Boyer, R., Stenroos, E.S., Chandrasekharappa, S., Athanassiadou, A., Papapetropoulos, T., Johnson, W.G., Lazzarini, A.M., Duvoisin, R.C., Di Iorio, G., Golbe, L.I., Nussbaum, R.L., 1997. Mutation in the alpha-synuclein gene identified in families with Parkinson's disease. Science 276, 2045–2047.

Rink, E., Wullimann, M.F., 2004. Connections of the ventral telencephalon (subpallium) in the zebrafish (*Danio rerio*). Brain Res. 1011, 206–220.

Rogaeva, E., Johnson, J., Lang, A.E., Gulick, C., Gwinn-Hardy, K., Kawarai, T., Sato, C., Morgan, A., Werner, J., Nussbaum, R., Petit, A., Okun, M.S., McInerney, A., Mandel, R., Groen, J.L., Fernandez, H.H., Postuma, R., Foote, K.D., Salehi-Rad, S., Liang, Y., Reimsnider, S., Tandon, A., Hardy, J., St George-Hyslop, P., Singleton, A.B., 2004. Analysis of the PINK1 gene in a large cohort of cases with Parkinson disease. Arch. Neurol. 61, 1898–1904.

Rose, S., Nomoto, M., Jenner, P., Marsden, C.D., 1989. Transient depletion of nucleus accumbens dopamine content may contribute to initial akinesia induced by MPTP in common marmosets. Biochem. Pharmacol. 38, 3677–3681.

Sallinen, V., Torkko, V., Sundvik, M., Reenilä, I., Khrustalyov, D., Kaslin, J., Panula, P., 2009. MPTP and MPP+ target specific aminergic cell populations in larval zebrafish. J. Neurochem. 108, 719–731.

Shimamura, K., Takeichi, M., 1992. Local and transient expression of E-cadherin involved in mouse embryonic brain morphogenesis. Development 116, 1011–1019.

Taniguchi, Y., Takeda, S., Furutani-Seiki, M., Kamei, Y., Todo, T., Sasado, T., Deguchi, T., Kondoh, H., Mudde, J., Yamazoe, M., Hidaka, M., Mitani, H., Toyoda, A., Sakaki, Y., Plasterk, R.H., Cuppen, E., 2006. Generation of medaka gene knockout models by target-selected mutagenesis. Genome Biol. 7, R116.

Valente, E.M., Abou-Sleiman, P.M., Caputo, V., Muqit, M.M., Harvey, K., Gispert, S., Ali, Z., Del Turco, D., Bentivoglio, A.R., Healy, D.G., Albanese, A., Nussbaum, R., González-Maldonado, R., Deller, T., Salvi, S., Cortelli, P., Gilks, W.P., Latchman, D.S., Harvey, R.J., Dallapiccola, B., Auburger, G., Wood, N.W., 2004. Hereditary early-onset Parkinson's disease caused by mutations in PINK1. Science 304, 1158–1160.

van Ham, T.J., Thijssen, K.L., Breitling, R., Hofstra, R.M., Plasterk, R.H., Nollen, E.A., 2008. *C. elegans* model identifies genetic modifiers of alpha-synuclein inclusion formation during aging. PLoS Genet. 4, e1000027.

Wen, L., Wei, W., Gu, W., Huang, P., Ren, X., Zhang, Z., Zhu, Z., Lin, S., Zhang, B., 2008. Visualization of monoaminergic neurons and neurotoxicity of MPTP in live transgenic zebrafish. Dev. Biol. 314, 84–92.

Wittbrodt, J., Shima, A., Schartl, M., 2002. Medaka—a model organism from the far east. Nat. Rev. Genet. 3, 53–64.

Yang, H., Tiersch, T.R., 2009. Current status of sperm cryopreservation in biomedical research fish models: zebrafish, medaka, and Xiphophorus. Comp. Biochem. Physiol. C: Toxicol. Pharmacol. 149, 224–232.

Zimprich, A., Biskup, S., Leitner, P., Lichtner, P., Farrer, M., Lincoln, S., Kachergus, J., Hulihan, M., Uitti, R.J., Calne, D.B., Stoessl, A.J., Pfeiffer, R.F., Patenge, N., Carbajal, I.C., Vieregge, P., Asmus, F., Müller-Myhsok, B., Dickson, D.W., Meitinger, T., Strom, T.M., Wszolek, Z.K., Gasser, T., 2004. Mutations in LRRK2 cause autosomal-dominant parkinsonism with pleomorphic pathology. Neuron 44, 601–607.

Zupanc, G.K., 2008. Adult neurogenesis and neuronal regeneration in the brain of teleost fish. J. Physiol. Paris 102, 357–373.